AN INVESTIGATION OF STRAIN AGING IN FATIGUE

by
J. C. Levy and G. M. Sinclair

A Research Project of the
DEPARTMENT OF THEORETICAL AND APPLIED MECHANICS
UNIVERSITY OF ILLINOIS

Sponsored by
OFFICE OF NAVAL RESEARCH, U. S. NAVY
Contract N6-ori-071(04), Project NR-031-005
TECHNICAL REPORT NO. 39

Urbana, Illinois
August, 1954

TECHNICAL REPORT NO. 39
on a research project entitled
THE BEHAVIOR OF MATERIALS
UNDER REPEATED STRESS
Project Supervisor, T. J. Dolan

AN INVESTIGATION OF STRAIN AGING IN FATIGUE

J. C. Levy
Graduate Research Assistant

G. M. Sinclair
Research Associate Professor

DEPARTMENT OF THEORETICAL AND APPLIED MECHANICS
UNIVERSITY OF ILLINOIS

TABLE OF CONTENTS

Chapter		Page
	ABSTRACT	ii
	ACKNOWLEDGMENT	v
I	INTRODUCTION	1
	1. Preliminary	1
	2. Purpose of Investigation	2
	3. Scope of Tests	3
II	TEST APPARATUS AND PROCEDURE	4
	1. Material Used and Preparation of Specimens.	4
	2. The Testing Machine and Calibration	4
	3. Test Procedure	6
	4. Statistical Procedure	7
	(a) Means and Confidence Limits	7
	(b) Comparison Between Sets of Lives . . .	8
III	RESULTS AND DISCUSSION	10
	1. Microstructure	10
	2. Tensile Tests	10
	3. Fatigue Results	11
	(a) The Original Low Carbon Steel	11
	(b) Specimens with Carbon and Nitrogen Greatly Reduced	16
	(c) The Re-Nitrided Specimens	17
	4. General	18
IV	CONCLUSIONS	22
	APPENDIX A	24
V	THE DEFORMATION OF METALLIC CRYSTALS .	24
	1. Evidence from the Microscope	24
	2. The Dislocation Concept	26

TABLE OF CONTENTS (Continued)

Chapter		Page
VI	STRAIN AGING THEORY APPLIED TO FATIGUE.	28
	1. Strain Aging Effects in Tension	28
	2. Tensile Strain Aging Explained in Terms of Dislocation Theory	28
	3. Consideration of Repeated Load Conditions .	30
	4. Theories of Strain Aging Applied to Fatigue	
	(a) Nabarro's Work	31
	(b) Cottrell's Strain Aging Theory	36
	BIBLIOGRAPHY	41
	TABLES	
	FIGURES	

DISTRIBUTION LIST

Technical and Summary Reports

Contract N6-ori-071(04) Project NR-031-005

Chief of Naval Research
Attn: Code 423 (2)
Department of the Navy
Washington 25, D. C.

Director
Office of Naval Research
Branch Office
150 Causeway Street
Boston, Mass.

Director
Office of Naval Research
346 Broadway
New York 13, New York

Director
Office of Naval Research
Branch Office
The John Crerar Library Bldg.
Tenth Floor, 86 E. Randolph
Chicago 1, Illinois

Director
Office of Naval Research
Branch Office
1000 Geary Street
San Francisco 9, Calif.

Director
Office of Naval Research
Branch Office
1030 E. Green Street
Pasadena 1, Calif.

Contract Administrator, SE Area
Attn: Mr. R. F. Lynch
Room 13, Staughton Hall
c/o George Washington University
Washington 6, D. C.

Director
Attn: Technical Information Officer (9)
Naval Research Laboratory
Washington 25, D. C.

U.S. Naval Engineering Exp. Station
Attn: Metals Laboratory
Annapolis, Maryland

Assistant Naval Attache for
Research (2)
Office of Naval Research
Branch Office
Navy 100
c/o Fleet Post Office
New York, N. Y.

Director, Naval Research Laboratory
Attn: Code 3500, Metallurgy Div. (1)
Code 2020, Tech. Library (1)
Washington 25, D. C.

Bureau of Aeronautics
Attn: N. E. Promisel, AE-41 (3)
Technical Library TD-41 (1)
Department of the Navy
Washington 25, D. C.

Commanding Officer
Naval Air Material Center
Attn: Aero. Materials Lab.
Naval Base Station
Philadelphia, Pa.

Bureau of Ordnance
Attn: Rex
Technical Library, Ad3
Department of the Navy
Washington 25, D. C.

Superintendent, Naval Gun Factory
Attn: Metallurgical Lab, DE 713
Washington 25, D. C.

Commanding Officer
U. S. Naval Ordnance Laboratory
White Oaks, Maryland

Commanding Officer
U. S. Naval Ordnance Test Station
Inyokern, Calif.

Wright Air Development Center
Attn: Materials Laboratory
Flight Research Lab (WCRRL)
Wright-Patterson Air Force Base
Ohio

Iowa State College
Attn: Dr. F. H. Spedding
P. O. Box 14A, Station A
Ames, Iowa

Knolls Atomic Power Laboratory
Attn: Document Librarian
P. O. Box 1072
Schenectady, New York

Los Alamos Scientific Laboratory
Attn: Document Custodian
P. O. Box 1663
Los Alamos, New Mexico

Mound Laboratory
Attn: Dr. M. M. Haring
U. S. Atomic Energy Commission
P. O. Box 32
Miamisburg, Ohio

U. S. Atomic Energy Commission
New York Operations Office
Attn: Div. of Technical Information
& Declassification Service
P. O. Box 30, Ansonia Station
New York 23, N. Y.

Oak Ridge National Laboratory
Attn: Central Files
P. O. Box P
Oak Ridge, Tenn.

Sandia Corporation
Sandia Base
Attn: Mr. Dale M. Evans,
Document Division
Albuquerque, New Mexico

U. S Atomic Energy Commission
Library Branch, Tech. Information
Service, ORE
P. O. Box E
Oak Ridge, Tenn.

Dr. Alfred M. Freudenthal
1044 Madison Avenue
New York 21, New York

Brown University
Attn: W. Prager
Providence, R.I.

Dr. I. R. Jackson
Battelle Memorial Institute
505 King Avenue
Columbus, 1, Ohio

Westinghouse Electric Corporation
Atomic Power Division
Attn: Librarian
P. O. Box 1468
Pittsburgh 30, Pa.

Dr. R. F. Mehl
Carnegie Institute of Technology
Metals Research Laboratory
Schenley Park
Pittsburgh 13, Pa.

Mr. R. E. Peterson, Chairman
ASTM Committee E-9 on Fatigue
Westinghouse Research Laboratories
East Pittsburgh, Pa.

Dr. C. S. Smith
Institute for the Study of Metals
University of Chicago
Chicago, Illinois

Mr. J. L. Bates
Managing Director
Technical Department
Maritime Commission
Washington, D. C.

Director
David Taylor Model Basin
Department of the Navy
Washington 7, D. C.

Dr. Finn Jonassen
National Academy of Sciences
2101 Constitution Ave., N. W.
Washington, D. C.

Commanding Officer
U. S. Naval Proving Ground
Attn: Laboratory Division
Dahlgren, Virginia

Professor B. J. Lazan
Dept. of Mechanical Engineering
University of Minnesota
Minneapolis, Minn.

Case Institute of Technology
Metals Research Laboratory
Attn: Mr. L. J. Ebert
Cleveland, Ohio

National Advisory Comm. for Aeronautics
Structures Research Division
Attn: R. F. Hardrath
Langley Air Force Base, Virginia

Bureau of Ships
Attn: Code 343 (3)
Code 337L, Technical Library (1)
Department of the Navy
Washington 25, D. C.

Director, Materials Laboratory
Building 291
Attn: Code 907
New York Naval Shipyard
Brooklyn 1, New York

Bureau of Yards and Docks
Department of the Navy
Washington 25, D. C.

Post Graduate School
Attn: Dept. of Metallurgy
U. S. Naval Academy
Monterey, California

Chief of Staff, U.S. Army
Attn: Director of Research and Development
The Pentagon
Washington 25, D. C.

Office of the Chief of Ordnance
Research and Development Service
Attn: ORDTB (3)
Department of the Army
Washington 25, D. C.

Commanding Officer
Watertown Arsenal
Attn: Laboratory Division
Watertown, Mass.

Commanding Officer
Frankford Arsenal
Attn: Laboratory Division
Frankford, Pennsylvania

Office of the Chief of Engineers
Attn: Research and Development Branch
Department of the Army
Washington 25, D. C.

General Electric Company
Technical Services Division
Technical Information Group
Attn: Miss M. G. Freidank
P. O. Box 100
Richland, Washington

Commanding Officer
Office of Ordnance Research
Attn: Metallurgy Division
Duke University
Durham, North Carolina

Atomic Energy Commission
Division of Research
Metallurgical Branch
Washington 25, D. C.

National Bureau of Standards
Attn: Physical Metallurgy Division
Washington 25, D. C.

National Advisory Committee for Aeronautics
1724 F Street, N. W.
Washington 25, D. C.

Argonne National Laboratory
Attn: Dr. Hoylande D. Young
P. O. Box 5207
Chicago 80, Illinois

U. S. Atomic Energy Commission
Attn: B. M. Fry
1901 Constitution Ave., N. W.
Washington 25, D. C.

Brookhaven National Laboratory
Technical Information Division
Attn: Research Library
Upton, Long Island, N. Y.

Carbide & Carbon Chemicals Div.
Plant Records Department
Central Files (K-25)
P. O. Box P
Oak Ridge, Tenn.

Carbide & Carbon Chemicals Div.
Central Reports & Information Office (Y-12)
P. O. Box P
Oak Ridge, Tenn.

University of California
Radiation Laboratory
Information Division
Room 128, Building 50
Attn: Dr. R. K. Wakerling
Berkeley, California

National Advisory Comm. for Aeronautics
Aircraft Engine Laboratory
Cleveland Airport
Attn: Library
Cleveland 11, Ohio

University of California
Attn: J. E. Dorn
Berkeley, California

Welding Research Council
Attn: Mr. W. Spraragen
29 West 39th Street
New York, New York

Chief of Naval Research
c/o Navy Research Section
Library of Congress
Washington 25, D. C.

Central Air Documents Office (2)
CADO-F1
Wright-Patterson Air Force Base
Ohio

Air Materiel Command
Attn: Materials Laboratory
WCRTS (2)
Wright-Patterson Air Force Base
Ohio

ABSTRACT

Fatigue tests were performed on low carbon steel at a rate of 2,600 load cycles per minute and at temperatures up to 700° F. All tests were conducted at a constant stress amplitude of 35,000 lb. per sq. inch. A number of specimens, usually 10, were tested at each selected temperature, and the results were analyzed statistically. It was found that a peak occurred in fatigue life in the region of 450° F. There was a pronounced tendency for the scatter in life to increase as the mean life increased.

Subsequent tests established that the magnitude of the observed peak depended on the amount of carbon and nitrogen in solid solution so that the effect could logically be classified as one of strain aging which takes place during the course of the test. When both carbon and nitrogen were present the peaking temperature was somewhat higher than when nitrogen alone was present, which seemed to indicate an interaction between the two types of interstitial atoms.

A recently developed theory of strain aging has been applied in which carbon and nitrogen atoms are presumed to strengthen the metal by diffusing to dislocations in the crystal lattice. To apply this theory to fatigue conditions, the following assumptions were made:

(1) The time available for aging was of the same order as the time of one loading cycle.

(2) The distance to be travelled by the carbon and nitrogen atoms, in order to re-anchor dislocations in fatigue affected zones, was 2×10^{-6} cm. (This corresponds to the distance they travel under tensile conditions and approximates to the closest approach of dislocations in a heavily cold worked metal.)

Utilizing these assumptions, the calculated peaking temperature agreed well with the observed value. A curve was constructed of the predicted temperature for peak life over a wide range of cyclic rates.

ACKNOWLEDGMENT

This investigation has been conducted in the research laboratories of the Department of Theoretical and Applied Mechanics as part of the work of the Engineering Experiment Station, University of Illinois, in cooperation with the Office of Naval Research, U. S. Navy, under Contract N6-ori-071(04). The advice and criticism of Professor T. J. Dolan, who is Head of the Department, and of Professor H. T. Corten is greatly appreciated. Acknowledgment is also due to D. Bailey, G. Mercer, R. Bennett and W. B. Whitler, who assisted in various phases of the project.

I INTRODUCTION

1. Preliminary

The term strain aging is familiar in connection with the recovery of the yield point in mild steel after tensile overstraining and there are other instances in which it is known to exert an appreciable effect on mechanical properties. For example, steel exhibits a greater tensile strength at mildly elevated temperatures than it does at room temperature; this is attributable to strain aging occurring during the course of the test. As to the origin of strain aging, it has been known for a number of years that it is directly connected with the presence of carbon and nitrogen in the steel. Under suitable circumstances, extremely small amounts of either element are sufficient to produce the effect. * (1) (2) During conditions of repeated loading there are certain types of behavior which have lately been associated with the aging of affected portions of the material. Sinclair (3) has shown that materials capable of strain aging may readily be "coaxed" (i. e. run for large numbers of cycles at several successively increasing values of stress) to a much higher fatigue strength than they formerly possessed. Again, when such materials are tested by the Prot method, to establish their endurance limits, the results may be affected by aging occurring while the test is in progress. (4)

The development of fatigue damage is, by its nature, a relatively long time phenomenon during which plastic deformation occurs in highly localized regions. It is to be expected therefore that, if a material is capable of strain aging, it will do so in these deformed regions when subjected to repeated loading.

* Numbers in parentheses refer to bibliography.

There appear to have been no attempts to correlate quantitative knowledge of strain aging with knowledge of fatigue properties. Such a project was thought to be attractive because of recent advances in the theory of strain aging made by researchers in the field of metal physics.

2. Purpose of Investigation

The observation that some steels, notably those in the low carbon category, appear to have greater fatigue strength in the range 400 to 500°F than at room temperature has been reported by several investigators.[5][6] The purpose of the present work was to investigate this elevated temperature behavior using statistical methods which lend assurance to the analysis of results. The eventual aim was to compare, both qualitatively and quantitatively, the observed elevated temperature behavior with that deduced from strain aging theory.

From the qualitative standpoint the aim was to isolate the effect of strain aging on fatigue life by modifying the carbon and nitrogen contents of the metal. Quantitatively any basic correlation between fatigue strength and strain aging properties necessarily involves the comparison of experimental fatigue results with the predictions of strain aging theory, so that the purpose of this part of the investigation was:

(1) To suggest methods for utilizing strain aging theory to take account of repeated loading conditions. This part of the work is contained in Appendix A.

(2) To examine the agreement between theoretical and experimental results in order to assess the validity of the application of strain aging theory to this problem and, by inference, to other aging phenomena such as coaxing, the effect of rest periods on fatigue performance, the occurrence of a sharp "knee" in the S-N diagram, etc.

3. Scope of Tests

Three batches of metal were tested in reversed bending at selected temperatures up to about 700°F. The first batch consisted of ordinary low carbon steel, the second batch was of the same steel treated so as to reduce the carbon and nitrogen contents and hence minimize the strain aging effects. The third batch was given the same treatment as the second but was also given a subsequent treatment to restore nitrogen to the lattice and therefore to reintroduce strain aging ability. The same cyclic loading rate was used for all tests.

It was decided not to try to establish the endurance limit for each batch at each selected temperature because of the length of time and quantity of specimens required for such an operation. Instead, a stress of 35,000 lb. per sq. inch, (which was above the endurance limit at room temperature) was chosen, and all specimens were run at this nominal stress. The performance was judged on the basis of the number of cycles to fracture.

To provide sufficient data for reliable statistical comparison of the mean life at one temperature with that at another, a number of specimens (usually 10) were tested under each chosen condition. As a subsidiary phase of the work an examination was made of the variability in fatigue life through the temperature range.

II TEST APPARATUS AND PROCEDURE

1. Material Used and Preparation of Specimens

The material used for the series of tests was a 1/4" diameter SAE 1018 cold rolled rod having the following nominal chemical composition:

C	Mn	P	S
0. 15-0. 20	0. 60-0. 90	0. 04 max	0. 05 max.

The specimens were machined to the form and dimensions shown in Fig. 1. The reduced sections were polished longitudinally with No. 1/0 followed by No. 2/0 emery polishing paper.

Subsequent heat treatment was of three kinds:

Batch I — Heated in an inert atmosphere of helium at 1300°F for 24 hours then furnace cooled.

Batch II — Heated in an atmosphere of wet hydrogen at 1300°F for four days. The purpose of this treatment was to reduce the carbon and nitrogen content of the steel and thus to minimize the strain aging properties of the material.

Batch III — Same treatment as Batch II but the specimens were reheated to 1300°F for 24 hours in an atmosphere of ammonia and again furnace cooled, the purpose being to reintroduce nitrogen and hence strain aging characteristics to the steel.

In order to determine the success of the various heat treatments, a sample from each batch was polished and etched and microphotographs (x150) of the various crystalline structures were prepared.

2. Testing Machine and Calibration

The fatigue tests were carried out on the specially-built rotating beam machine shown in Fig. 2. The beam was simply supported at the

ends and loaded by dead weights at the third points so that there was a constant bending moment over the central section. The grips were machined to accommodate a 1/4" diameter specimen and drive was provided by an electric motor through a belt and pulley arrangement giving the machine a speed of 2,600 revolutions per minute.

The machine was calibrated for load by measuring, weighing and balancing the separate parts. The bending moment at the test section due to the tare weight of the machine was then calculated and the result taken into account in computing the magnitude of extra weights to be added to obtain the specified stress at the test section.

The temperature of the specimen was controlled by means of an electric furnace fitted over the central portion of the beam. Current to the furnace was regulated by a Leeds and Northrup "Micromax" temperature regulator and recorder. Automatic shut-off of electricity, on breakage of specimen, was provided by arranging for the falling beam to trip a microswitch connected into both the heating and motor circuits. The electrical connections are shown in Fig. 3 and it will be seen that the heating and motor circuits could be operated separately when the microswitch was "on" but when this switch was "off," both circuits were dead. This arrangement allowed the specimen to be brought up to a predetermined temperature before the fatigue loading was initiated.

Temperature calibration was carried out by placing a specimen in position with a thermocouple spot-welded to the test section, the leads being connected to a potentiometer. With the furnace closed, simultaneous readings were taken of furnace temperature, as indicated on the "Micromax" recorder, and the thermocouple e. m. f. as indicated on the potentiometer. The corresponding temperature at the surface of the specimen was then found from the e. m. f. reading

When the furnace was fully up to its pre-set temperature, the potentiometer readings continued to be taken until the specimen temperature attained its maximum value. It was found that this took approximately thirty minutes, a length of time which was nearly constant for several different furnace temperatures.

3. Test Procedure

Exploratory tensile tests were carried out after the various heat treatments had been completed, the specially machined tensile specimens having been heat treated with the various batches of material. The data on these tests are given in the next section.

For the fatigue tests the diamter of the minimum section of the specimen was measured with a hand ball-point micrometer and the load calculated to give the desired nominal stress at the minimum section according to the ordinary flexure formula,

$$S = Mc/I$$

Where:

S = the stress at the outer fiber in lb. per sq. inch.

M = the bending moment applied in lb. inches.

I/c = the section modulus at the critical section in inches^3.

After the specimen had been mounted in the machine, the concentricity of the assembly was verified by the use of an Ames dial gage. Supports were placed under the beam to prevent bending of the specimen while it was being heated and, with the furnace closed, the heating circuit was switched on After the furnace was up to the pre-set temperature, thirty minutes were allowed for the specimen to reach thermal equilibrium. The motor circuit was then switched on, the supports removed and the machine loaded.

4. Statistical Procedure

All statistical calculations were based on the assumption of a log-normal distribution for cyclic lifetimes under any particular set of conditions. That such a distribution is approximately valid has often been observed. [7] Since only about ten specimens were tested under each condition a "small sample" analysis was employed. One of the sources containing work of this kind is a book by Brownlee. [8]

(a) Means and Confidence Limits

The mean of each set of results was calculated as the number of cycles corresponding to the mean value of log N

$$\text{i.e.} \qquad \log \bar{N} = \frac{\Sigma (\log N)}{n} \qquad (1)$$

Where $\bar{N}$ = required mean value of fatigue life

N = number of cycles to fracture

n = number of specimens in the set

Σ denotes summation

The confidence limits for any set of results specify the range within which there is a certain probability of finding the true value of the mean as determined by the sample and according to the distribution law which has been assumed. For example, there is a 0.95 probability that the mean of the true population will lie within the 95% confidence limits to be established here.

Let the upper and lower confidence limits be Nu and N_L respectively. Then,

$$\log Nu = \log \bar{N} + \frac{t\sigma}{\sqrt{n}} \qquad (2)$$

$$\log N_L = \log \bar{N} - \frac{t\sigma}{\sqrt{n}} \qquad (3)$$

Where σ = standard deviation of the set

i.e. $$\sigma = \sqrt{\frac{\sum(\log \bar{N} - \log N)^2}{n - 1}}$$

and t is a quantity known as "Student's t" for which tables are available according to the number of "degrees of freedom". For comparison in which a relatively small number of specimens are being tested, the number of degrees of freedom is one less than the number of specimens. In this report we shall primarily be concerned with 4, 9 and 18 degrees of freedom. Values of "t" for these degrees are given in Table I for different levels of significant difference.

(b) Comparison between Sets of Lives

Since the investigation was concerned with the detection of strengthening due to strain aging, it was necessary to decide whether the results at one temperature were significantly different from those at another, i.e., to estimate the chance of the two sets being drawn from the same population.

The method used in this report was to compare the means of the two sets through the value of Student's "t" in order to establish the level of significant difference between them. Subscripts 1 and 2 refer to the two sets of results which are being compared.

For this case "t" is defined by:

$$t = \frac{\log \bar{N}_1 - \log \bar{N}_2}{\lambda} \sqrt{\frac{n_1 n_2}{n_1 + n_2}} \qquad (4)$$

Where $$\lambda^2 = \frac{\sum(\log N_1)^2 - \frac{(\sum \log N_1)^2}{n_1} + \sum(\log N_2)^2 - \frac{(\sum \log N_2)^2}{n_2}}{n_1 + n_2 - 2}$$

$$= \frac{X_1 + X_2}{n_1 + n_2 - 2} \qquad \text{for convenience} \qquad (5)$$

Where X_1 and X_2 respectively are the first and second pairs of terms in the numerator of the line above.

When the value of t in Equation 4 has been determined, Table I is entered at $(n_1 + n_2 - 2)$ degrees of freedom to determine the level of significant difference between the means of the two sets. If, for example, the value of t was 2.00, the number of degrees of freedom being 18, there would be a significant difference at the 10% level but not at the 5% level which requires a value of t of at least 2.10. The conclusion would then be that there was a 0.9 probability that the sets of lives were drawn from different populations

III RESULTS AND DISCUSSION

1. Microstructure

A photomicrograph (x150) of the material in the "as received" condition is shown in Fig. 4. In Figs. 5 to 7 are shown the material designated as Batches I, II and III respectively.

In Fig. 5 it will be seen that ample carbon was present in Batch I to cause strain aging effects while in Fig. 6 the lower concentration of carbon in Batch II is confirmed by the absence of pearlite. Nitride needles may be seen in Fig. 7 indicating that sufficient nitrogen had been re-introduced to Batch III to cause strain aging properties to reappear.

2. Tensile Tests

Tensile stress-strain curves for the three batches of material are shown in Fig. 8. The early portions are reproduced to a more convenient scale in Fig. 9.

Batch I shows the characteristic 2% plastic elongation at the yield point of low carbon steel. The value of the yield point was 27,500 lb. per sq. inch and the ultimate stress was 56,000 lb. per sq. inch, the total elongation on a 1 inch gage length being 40%.

In Batch II there was little, if any, indication of a yield point. The 0.2% yield strength was 24,000 lb. per sq. inch, the ultimate stress was 48,200 lb. per sq. inch and the total elongation on a 1 inch gage length was 33%. The disappearance of the sharp yield point is a consequence of the removal of carbon and nitrogen and is consistent with the strain aging concept described in Appendix A.

There is a small but definite plastic elongation at the yield point in the stress-strain curve for Batch III. Again this is consistent with the return of strain aging properties. The yield point was 29,600 lb. per sq.

inch and the ultimate stress was 56,400 lb. per sq. inch. The total elongation on a 1 inch gage length was 37%.

3. Fatigue Results

All fatigue tests were run in the rotating beam machine at a speed of approximately 2,600 r. p. m. and at a nominal stress of 35,000 lb. per sq. inch. The number of cycles to failure of each specimen is shown in Table II and the data are plotted in Figs. 10, 11 and 12 for Batches I, II and III respectively. In these figures are also marked the value of $\log \overline{N}$ and the 95% confidence limits for each set of results. These are denoted in each case by three short horizontal lines, the middle one representing the value of $\log \overline{N}$, the other two the upper and lower confidence limits. The numerical values are computed in Table III, according to the method previously outlined.

(a) The Original Low Carbon Steel (Batch I)

The confidence which may be placed in the apparent peak in fatigue life (Fig. 10) is readily assessed by means of the statistical work presented in Table IV. Comparing, in turn, the sets of lives at 220°F, 300°F and 420°F with the set of lives at room temperature, the table shows that there exists, in all cases, a 5% level of significant difference between the means. This may be interpreted as saying that there is only one chance in twenty that the lives of the specimens at any of the three elevated temperatures were drawn from the same population as the lives at room temperature. Comparing the actual life values, it may then be concluded that, for these four different temperatures, the shortest life occurred at room temperature.

Again comparing, in turn, the lives at room temperature, 220°F and 300°F with the lives at 420°F, it is found that, in all cases, a significant

difference between means exists at the 5% level. Hence it may further be concluded that, of the four sets of values, the mean life at 420°F was the greatest.

An important point here is that two specimens tested at 420°F did not break at more than 3 million cycles but the statistical work has been carried out on the assumption that failure took place when the machine was stopped. Thus calculations involving the comparison between the mean life at 420°F and the mean life at some other temperature are bound to err on the conservative side, the true mean life at 420°F being greater than that shown in Fig. 10.

Turning now to the data at 530°F and 700°F and comparing these sets of lives with that at 420°F, it is found that there is, in all cases, a significant difference between means at the 5% level. Hence the life at 700°F was shorter than the life at 530°F which in turn was shorter than that at 420°F.

In summary of Fig. 10, it may be concluded that the fatigue life of the material was greater at 420°F than at room temperature and that the lives at 220°F and 300°F had intermediate values. At temperatures higher than that at which the peak life occurred there was a steady drop in life as shown by the data at 530°F and 700°F.

An attempt was made to estimate the exact value of the peaking temperature by drawing straight lines through the mean log lives in Fig. 10 at the various testing temperatures. It may be seen that the value of temperature corresponding to maximum life is approximately 460°F. If we estimate the error in temperature calibration of the specimen as $\pm$ 25°F, the range 435° - 485°F is arrived at for the peaking temperature.

This range of temperature may be compared with the predictions of the theoretical treatments developed in Appendix A. These are based on the hypothesis that the temperature at which maximum life occurs is determined by the rate at which dissolved carbon and nitrogen atoms segregate to dislocations in fatigue affected zones.

The first of the theoretical treatments (after Nabarro, see Appendix A) assumes that the carbon and nitrogen atoms have to travel a distance of 2×10^{-6} cm. during the aging process. Fig. 18 shows $\log_{10} t^{-1}$ plotted against $\frac{1000}{T}$ where t is the time available for aging and T is the absolute (Kelvin) temperature. If t is equal to the time for a single load cycle to be applied then, at 2,600 cycles per minute the corresponding temperature in Fig. 18 is 500°F for both carbon and nitrogen. This temperature agrees well with the observed peak.

The second of the theoretical treatments (after Cottrell, see Appendix A) describes the manner and path by which the interstitial atoms move in reaching dislocations. As shown in the appendix, the maximum aging effect is forecast in the range 385°F to 585°F when the diffusing atoms are nitrogen. Again this agrees well with the experimental peaking range of 435° - 485°F. With carbon as the diffusing atom the predicted peaking range is considerably higher and this seeming discrepancy will be referred to later.

It may be well to emphasize that both mechanisms essentially describe different aspects of the same phenomenon. Cottrell's was developed from a fairly rigorous mathematical treatment but tells nothing directly about the size of domain involved. On the other hand, Nabarro's work suggests that the average interstitial atom moves a distance of the order of 2×10^{-6} cm. but tells nothing about the distribution or availability of the interstitial atoms. It is interesting to note that the stated distance is

identical with the thickness of the individual lamellae in the picture of slip in aluminum (Fig. 13) observed by Heidenreich and Shockley. This size of domain also is comparable to the so-called "limiting fragment size"[9] or the closest approach between dislocations in a heavily cold worked zone. It appears then that the process of aging is one of diffusion to a dislocation from the fragments of linear dimension 2×10^{-6} cm. immediately adjacent to the dislocation.

Although much of the work on the deformation of metallic crystals has been established on the strength of electron microscope observations of aluminum, a structure of both fine and coarse slip lines has lately been observed in iron by Paxton, Adams and Massalski.[10] In common with aluminum, copper, lead and gold the formation of the slip lines was sensitive to the state of preparation of the surface. Whether the lamellae in iron are the same thickness as those in aluminum and are displaced by the same amount is not known. In any case the validity of the diffusion calculations, and of the strain aging model is not critically dependent on the exact mode of slip within the crystal.

In comparing the theoretical predictions with the experimental results there is another point which should be noted. The theory predicts that, as temperature is increased, life will increase up to a maximum because of the larger number of dislocations being re-anchored at the higher temperatures. It might be expected then that, when some maximum strength has been reached, the fatigue life would be constant over a certain range of temperature since, if the interstitials have time to re-pin the dislocations at say 500°F, they have ample time to do so at 550°F. However, it will be observed in Fig. 10 that immediately after the peak was reached there was an extremely sharp drop in life. Two possible reasons suggest

themselves for this decrease. The first is that, as soon as the maximum possible strengthening effect due to aging has been realized, the weakening indicated by the continuous drop in yield strength with increase in temperature begins to be evident. The second is that when the peaking temperature is exceeded at a particular cyclic frequency the interstitial atoms are able to move about so freely that they no longer exert a significant restraining influence on the movement of dislocations. This would be analogous to the sharp internal friction peaks observed in torsion pendulum experiments.[11]

A margin of error of $\pm$ 25°F in the experimental apparatus has been assumed above. Agreement between predicted and actual results will also be dependent on the accuracy of values of constants in the theoretical equations. While the latest available data have been used (in Appendix A) in evaluating the equations, there is naturally the possibility that the values were somewhat in error.

The changes in the predicted peaking temperature brought about by altering the assumed values of the time t available for aging, of the distance x the interstitial atoms have to move and the activation energy ΔH of the diffusion process have been investigated in the appendix and are illustrated in Figs. 19 and 20. Even allowing moderately large variations for t, x and ΔH the predicted peaking values still fall in the same general range as that obtained experimentally. The method appears to be sensitive enough, however, to enable the conclusion to be drawn that diffusion from the interslip region (Fig. 13) is unlikely. The necessary value of 10^{-5} cm. for x gives a predicted peaking temperature of 750°F which differs by nearly 300°F from the experimental value of 460°F, a deviation which is well outside the range of experimental error (provided always that the value of ΔH has not been grossly overestimated).

So far as the value of $\underline{t}$ is concerned, it seems reasonable that a time of the order of the cyclic time is significant since a slipped plane would presumably be subjected to maximum attack once per cycle. No final conclusions can yet be drawn on this point, however, since it happens that the predicted peaking temperature is not greatly affected by variation of $\underline{t}$ alone. This is because, in Equation 9, time and temperature are related through an exponent.

(b) Specimens with Carbon and Nitrogen Greatly Reduced (Batch II)

These results are presented in Fig. 11. Statistical analysis (Table IV) shows that the mean life at 420°F was different from that at room temperature so that a peak life persisted in the material in the 400° - 500°F range. However, if the lives at 420°F are compared with the lives of Batch I at the same temperature, it is found that these two sets of lives were also different at the 5% level of significance. Hence there was a less pronounced peak in the wet hydrogen treated batch, occurring at about the same temperature as did the peak for the original material.

The tensile stress-strain curves of Figs. 8 and 9 show that a trace of yield point remained after the wet hydrogen treatment so it is logical to expect that the strain aging characteristics would not have been entirely removed. It is known from tensile experiments that traces of strain aging are present even when carbon and nitrogen are removed below the limit of ordinary chemical analysis. As little as 0.001% of these elements is sufficient to cause strain aging tendencies.

To explore this avenue further a few specimens were subjected to the wet hydrogen treatment in a glass tube furnace instead of in the steel pot which was previously employed. The aim was to secure a more thorough removal of carbon and nitrogen. Fatigue results for these half dozen specimens are denoted by triangles in Fig. 11. It will be seen

that the peak is now absent, there being a continuous drop in life from room temperature up to 420°F.

As carbon and nitrogen were removed from solution there was a progressive decrease of the peaking tendency in fatigue life. This is entirely consistent with the picture of strain aging being the responsible mechanism.

3. The Re-Nitrided Specimens (Batch III)

These fatigue results are shown in Fig. 12 where it will be seen that a strong peak in fatigue life was once more present but in the region of 300°F as compared with 460°F for the original material. There is little need to support this conclusion by statistical work. None of the five specimens which were run at 300°F broke, while those run at 420°F all had lives of less than two and a half million cycles. The room temperature performance for this material was very much the same as for the previous two batches so that a true peaking phenomenon was observed and not merely an all round increase in strength.

The strain aging theory indicates that a peak should re-occur on the reintroduction of nitrogen but the apparent shift in peaking temperature was an unexpected result. When it was observed, the calibration of the apparatus was checked but no adjustment was found to be necessary. Nabarro's work, as plotted in Fig. 18 lead to the expectation of nearly equal peaking temperatures for each of the two types of interstitial, especially at cyclic speeds in the region of 2,600 r. p. m. where the carbon and nitrogen lines run close together. However the experimental result indicated that when carbon and nitrogen were both present the peaking temperature was higher than when nitrogen alone was present.

Such a shift in peaking temperature might be accounted for by the existence of interaction between carbon and nitrogen atoms when both are present in the iron lattice. Wert,[11] using internal friction measure-

ments, has concluded that the rate of aging of one type of interstitial is influenced by the presence of the other. At 110°C he found that the presence of nitrogen caused carbon to precipitate 2-1/2 times faster than it otherwise would. Again Fast [12] has found differences in behavior between iron containing nitrogen and iron containing carbon. For example, the Charpy impact value of technical iron shows a minimum at temperatures between 750°F and 930°F but there is no such minimum when carbon is the only impurity in the iron. With nitrogen as the impurity, there again is a minimum value in this temperature range. The difference in the critical temperature ranges for impact and fatigue might be accounted for by the higher rate of strain in the impact test.

It is interesting that calculations, based on Cottrell's work, which are presented graphically in Figs. 22 and 23 predict a difference in peaking temperature between nitrogen and carbon if they are separately present. Where nitrogen should cause a peak in fatigue life between 380°F and 580°F, carbon should not cause a peak in life until the range 700° - 1,100°F. The difference is due mainly to the greater solubility of nitrogen at lower temperatures.

Possibly then the experimentally observed peak was in reality due to nitrogen, the effect being strengthened by the premature precipitation of carbon. More experimental work is needed to distinguish finally between the separate and combined aging effects of the two elements.

4. General

The results suggest that mildly elevated operating temperatures are beneficial to fatigue resistance as far as low carbon steel is concerned. The best operating temperature is, by the argument pursued in the appendix, dependent on the frequency of the fatigue loading; in Fig. 24 are shown the

theoretical temperatures for best performance at frequencies from 60,000 to 10 cycles per minute. This curve is based on Equation 10 and so, in the light of the experimental results obtained, may give temperatures which are slightly too high. Also, at the higher temperatures, oxidation may become an important factor and there may be other changes in the metal which could prevent the formation of a relative peak.

It is noteworthy that, in general, as the mean fatigue life increases so does the scatter about the mean. This applies to each of the three different batches of material and is revealed by examination of the calculated values of standard deviation (Table III). Such a result is in agreement with previous observations on the width of scatter bands at different stress levels[7] in room temperature tests.

It is suggested that the variation in life observed in the present study may be interpreted in the following manner:

At constant stress amplitude the relative scatter in life is a function of the number of microscopic zones in which fatigue cracks are nucleated. If a large number of cracks are nucleated, they may grow together and hence result in a short life for the specimen. Nucleation and growth of a small number of cracks should result in a longer life. Thus, to a first approximation, the life may be said to be inversely related to the number of cracks nucleated in the plane of final failure. Due to the inhomogeneous character of real materials, there will be different numbers of cracks formed, at the same nominal stress, in individual specimens of a given sample. This variation will be reflected in larger scatter in life when the mean number of cracks is small because the percentage variation in the number of cracks is greater. At slightly elevated temperatures, the strain aging mechanism described in this paper has the effect of reducing

the mean number of cracks nucleated at a given stress, thus resulting in increased fatigue life accompanied by increased scatter in life. This argument appears to be in line with the experimental results obtained.

Even at room temperature some strain aging must occur during repeated loading and any picture of fatigue damage concerned with, say, low carbon steel should take this into account as a contributory feature. For example, the coaxing phenomenon, for materials which strain age, is to be expected. During coaxing[3] a low stress is applied for a large number of cycles (i.e., a long time) so that the affected zones are strengthened by aging. The stress is raised slightly and again a large number of cycles is run so that further strengthening of the same, or different, zones occurs. Thus the fatigue resistance is gradually increased by a progressive strengthening of the weakest portions and the subsequent inhibition of crack nucleation and growth. Again the increase in strength which occurs during rest periods after the repeated loading of ingot iron[13] may be accounted for by the aging of fatigued portions.

In the final analysis it must be kept in mind that all work in this report which has been characterized as "quantitative" might be more aptly described as "semi-quantitative" being based as it is on practical measurements of diffusion constants, solubility figures and moduli of rigidity besides the microscopically observed nature of crystal slip. Although a degree of success has been achieved in predicting the temperature at which peak fatigue life should occur for low carbon steel, the direct theoretical problem of predicting the magnitude of this peak life is another, much more complex question. Nevertheless, in this investigation an attempt has been made to apply to an engineering problem findings made in the more basic field of metal physics. It is believed that such correlations of different

fields of knowledge offer, as indeed they have in the past, a fruitful approach to the understanding of fundamental engineering science and therefore promise hope in the future of substantial advances in engineering practice.

IV CONCLUSIONS

The following conclusions may be drawn from the investigation:

1. The low carbon steel used in the tests exhibited considerably greater fatigue life in the region of 400°F to 500°F than it did at room temperature.
2. Subsequent tests showed that the increase in life could be attributed to the presence of carbon and nitrogen in the metal. The effect could therefore logically be classified as one of strain aging which occurs during the course of the test.
3. Calculations based on the assumption that the strengthening was caused by the diffusion of carbon and nitrogen atoms to dislocations which moved during local yielding predicted the peaking temperature closely, provided that:
   (a) The time available for aging to occur is of the order of the time to apply one load cycle.
   (b) The distance the carbon and nitrogen atoms have to travel to achieve aging during the fatigue process is the same as the distance they travel under tensile conditions, namely 2×10^{-6} cm. (Which also approximately corresponds to the "limiting fragment size," and to the closest approach of dislocations in a heavily cold worked metal)
4. Provided the theory, as developed, is substantially correct it is to be expected that the peaking temperature depends on cyclic rate. It should range from about 300°F for a rate of 10 cycles per minute up to about 700°F for 60,000 cycles per minute.
5. It appeared that when both nitrogen and carbon were present the peaking temperature was somewhat higher than when nitrogen

alone was present. The reason for this is not clear, but it may be that there is an interaction between the two kinds of atoms when both are present. There is an indication in one aspect of the theory that a higher peaking temperature is to be expected for carbon than for nitrogen when they are separately present.

6. At higher values of mean life there was, in general, an increase in the scatter of the results. This is consistent with the idea that the fewer the active damage spots, the wider is the scatter.

APPENDIX A

V DEFORMATION OF METALLIC CRYSTALS

While it is not the purpose of this part of the report to examine in detail the mechanism of slip and the allied phenomenon of work-hardening —processes which are, as yet, imperfectly understood—it will be useful to review certain ideas which have gained acceptance as helping the understanding of some of the observed changes in crystalline structure under load. More particularly, these ideas help to explain the production and growth of slip bands, and as such lead to the development of the strain aging theory to be described. Microscopic and other experimental evidence will be considered before an outline of the theoretical approach is given.

1. Evidence from the Microscope

When a metal is subjected to stress and its crystalline structure observed through a microscope at different stages of deformation, dark bands make their appearance and increase in number and thickness up to fracture. The bands are due to one layer or portion of a crystal slipping over the next, the sum total of these slippages being of the same order as the overall deformation of the material.

It is beyond the power of the light-microscope to resolve the internal structure of slip bands but, by use of the electron microscope, Heidenreich and Shockley[14] have shown that, in the case of aluminum, the bands are composed of clusters of lamellae (Fig. 13) whose thickness is about 200 Å. Each lamella has slipped relative to its neighbor by about 2000 Å, a distance which is remarkably constant for that metal. The motion is not one of pure translation, the lamellae being rotated through small angles relative to each other. The experiments have been repeated by other

workers with similar qualitative results for various metals, though none is so easy to deal with, or gives such consistent results, as aluminum. At this stage of development it is not possible to say whether the 2000 Å slip distance occurs all on one plane or whether there are contributions by a number of successive atomic planes. Brown[15] suggests that the region may consist of about 50 adjacent atomic planes each of which has slipped by several atomic distances.

The occurrence of slip bands in pure aluminum represents a fairly advanced stage of deformation, the first faint bands making their appearance when the strain is perhaps 0.025%. The spacing between the bands is then a few microns.

Previous to the inhomogeneous mode of deformation characterized by slip bands, the electron microscope indicates, according to Brown and Honeycombe,[16] that there exists a more homogeneous movement which has been called "micro-slip." The general domain undergoes deformation in which a great many atomic layers are moved relative to one another by a few atomic distances. At a certain stage slip bands make their appearance on a small number of favorable planes. Once created they seem to interact with each other since it is observed that fresh bands tend to appear midway between two existing ones. Deformation proceeds both by the creation of new bands and by the addition of lamellae to those already existing.

Slip bands are a feature of plastic deformation both under static loads and under fluctuating (fatigue) loads, but the modes of deformation are somewhat different in the two cases. Under tensile conditions, the creation of new bands seems to predominate, while in fatigue the broadening of bands formed early in the test is a salient feature. In fatigue, cracks eventually initiate within the slip bands.

2. The Dislocation Concept

Much present day theoretical work on the deformation of small metallic domains hinges on the concept of a dislocation. This term is used to refer to an imperfection in the atomic array originally conceived to account for the difference between the calculated and actual resistance to plastic deformation. The simplest type of dislocation may be thought of as an extra plane of atoms inserted on one side of a potential slip plane AB (Fig. 14). The material above AB is in compression, that below AB in tension. In an annealed metal it has been estimated that there are about 10^8 dislocations per square cm; in a heavily worked metal there are many more, possibly 10^{12} per square cm. The symbol $\perp$ is often used to denote a dislocation.

If now the dislocation moves across the crystal due to an applied shear stress, the material above AB slips one atomic distance over the material below AB. From this point of view therefore, the occurrence of slip may be regarded as a consequence of the movement of dislocations. Many of the effects observed in the microscope can, in fact, be explained in such terms. For instance, micro-slip may be described as an internal redistribution of dislocations which do not leave the surface until the stress is increased sufficiently to cause slip steps to form in preferred localities.

It has already been mentioned that these observed slip steps are of the order of 2000 Å or about 700 atomic distances and this number of dislocations cannot be assumed to be present on any one plane in the virgin lattice. A multiplication process for dislocations is therefore necessary and such a process is provided by the "Frank-Read Source." (17) (18) According to this mechanism large amounts of slip can take place on a single plane by the rotation of a dislocation about anchors provided by

dislocations in another atomic plane. This is shown diagramatically in Fig. 15 where the dislocation in the original position 1 is pinned at P and P'. Under the influence of an applied stress it bows into the successive positions 2, 3, 4, 5 so generating a new ring and leaving the original line PP' to repeat the operation. Alternatively, if a potential Frank-Read source is near the surface it may be pinned at only one point and a smaller force will be required to activate it than if the configuration is as depicted in Fig. 15.

Seitz [19] has suggested that active slip planes seize up because, after about 1000 dislocations have passed on one plane, the density of vacancies in that vicinity is very high. This causes strong distortion of the lattice which hinders the passage of further dislocations. Cottrell[20] and Brown[21] have made proposals utilizing Frank-Read sources to account for the lamellar nature of slip bands.

If the view is accepted of the dynamic behavior of dislocations being the root cause of slip and work hardening both in tension and in fatigue, it may thus be argued that the prevention or hinderance of the movement of dislocations will lead in turn to the retardation of the yielding process and the postponement of crack initiation. This will be recognized on the macroscopic level as increase in strength or fatigue life.

In the next section the proposition is developed that the mechanism of strain aging during fatigue provides, as it does during tension, just such a hinderance to dislocation movement and is, therefore, an effect which should be taken into account when fatigue properties are being evaluated.

VI STRAIN AGING THEORY APPLIED TO FATIGUE

1. Strain Aging Effects in Tension

If a mild steel specimen, possessing both upper and lower yield points, is strained into the plastic range and the stress is removed but is then immediately reimposed, (Fig. 16b) plastic deformation will continue at almost the same stress at which the test was interrupted. There will be no reoccurrence of a definite yield point. If, however, the material is left unloaded for a sufficient time and is subsequently reloaded, an upper and a lower yield point will once more be observed as shown in Fig. 16c.[22] Annealing at a mildly elevated temperature after straining greatly accelerates the return of the yield points.[23]

Increased hardness, increased tensile strength and decreased ductility accompany the return of the yield points and these effects are recognized as 'strain-aging'.

Besides accelerating the return of the yield point in an interrupted test, increased temperature has important effects during the course of an uninterrupted tensile test. As depicted in Fig. 17, mild steel shows an increase in ultimate strength at temperatures between 450°F and 550°F, due to strain aging during the test, in spite of decrease in yield strength.[24] It is to be noted, however, that the rate of straining modifies these results, the peak strength occurring at higher temperatures for higher strain rates.

2. Tensile Strain Aging Explained in Terms of Dislocation Theory

The most satisfactory explanation, at this time, of the occurrence of the upper yield point and of strain aging effects is that due to Cottrell.[25] According to his theory, small interstitial atoms (e. g. carbon and nitrogen in iron) tend to concentrate at the tensile side of dislocations in the crystal lattice since, in such positions, their energy is a minimum. From the

mechanical point of view, more space exists between atoms at the tensile side of a dislocation; this enables solute atoms to fit in more easily thus relieving the surrounding stress field. Once a particular solute atom occupies such a spot, energy barriers exist which make it difficult for a change of position to take place. This may be expressed by saying that there are attractive forces between dislocations and the clouds of interstitial atoms.

If crystal slip is regarded as a consequence of the movement of dislocations, it will be necessary, before slip can take place, for the force between dislocations and nearby solute atoms to be overcome. However, once this has occurred, a smaller force will be required to continue the movement of the freed dislocations which culminates in the slip process. Thus the theory gives a natural explanation of the two yield points encountered in strain aging materials. The effect is greatest in those lattices in which the interstitial atoms cause an anisotropic strain, e. g. in body-centered cubic systems such as α-iron.

If now, after yield has taken place, the material is unloaded but the load immediately re-applied, yielding will continue at the same stress at which the test was interrupted since the interstitial atoms have had no time in which to diffuse to the new dislocation sites.

If, however, the material is unloaded and allowed to rest for sufficient time to allow the interstitial atoms to diffuse and re-pin the dislocations, then upon reloading the two yield points will, once more, be in evidence.

Should the temperature during the rest period be raised, the carbon and nitrogen can diffuse at faster rates. Less time would then be required for the return of the yield points. As previously mentioned, this is exactly

the effect observed. Cottrell's model also accounts for the different peaking temperatures shown in Fig. 17 since at faster rates of straining there is less time for aging to occur and therefore a higher temperature is required for the maximum effect. Evidently then, the time required to obtain the maximum strain aging effect for given solute atoms in a given lattice depends upon the rate of diffusion (i. e., upon the temperature) and upon the distance to be travelled by the solute atoms.

3. Consideration of Repeated Load Conditions

In general, slip induced by cyclic stress is much more localized than slip caused by steadily applied stress. As has already been stated, slip under repeated load proceeds by the broadening of a few slip bands rather than by the formation of numbers of new bands as in tension. There are also other differences between the two types of deformation. For example slip bands formed during repeated stressing may start and end in the interior of a crystal whereas those formed by static tension almost invariably begin at a crystal boundary.

However, these differences do not invalidate the picture of slip and eventual crack initiation being the result of the dynamic behavior of dislocations. It should, therefore, be possible to utilize the mathematics of a valid tensile strain aging theory to account, both qualitatively and quantitatively, for certain variations in the fatigue life of strain aging materials, such as low carbon steel, at different temperatures and different rates of cyclic stress.

If aging is to help prevent further damage after initial slip, there are three major factors which will govern the process. These are (a) the time available for aging, (b) the distance the solute atoms have to travel in order to catch dislocations, and (c) the number of solute atoms required to achieve the pinning effect.

It seems reasonable to suppose that the time available for aging is of the same order as the time required for a single stress cycle to be imposed since, presumably, any particular atomic plane is subjected to maximum attack once per cycle.

The average distance to be travelled by the interstitial atoms is a difficult quantity to estimate, but again it seems reasonable, from the argument which has been developed, that the distance in fatigue is of the same order of magnitude as the distance under tensile conditions, about which more is known.

Some work[26] has previously been done towards the necessary weight percent of solute required to pin the density of dislocations present in a heavily worked zone and the results are used in one phase of the calculations which follow.

4. Theories of Strain Aging Applied to Fatigue

(a) Nabarro's Work

Nabarro[27] has carried out strain aging calculations based on a movement of carbon atoms in α- iron, after tensile overstraining, of 2×10^{-6} cm. and has shown good agreement with Muir's[28] experimental results on the time of recovery of yield point at various temperatures. However, values of diffusion coefficient and activation energy of carbon in iron were used which are not now the best available, and in the following work, values due to Wert[29] are utilized. The effect of the movement of nitrogen will also be considered.

The diffusion coefficient D of a diffusion process is defined by the equation:

$$J = -D \frac{\partial c}{\partial x} \qquad (6)$$

Where J = Quantity in grams of the diffusing substance which passes

per unit time through unit area of a plane at right angles to the direction of diffusion.

c = The concentration of the diffusing substance per unit volume (gr/c. c.)

x = Ordinate coinciding with the direction in which diffusion occurs.

D = Diffusion coefficient (cm^2/sec)

By a process of diffusion of interstitial atoms to dislocations, the order of the time $\underline{t}$ (in seconds) to achieve equilibrium in a pattern of linear dimensions $\underline{x}$ (centimeters) has been given by Nabarro[27] as:

$$t = \frac{x^2}{2D} \tag{7}$$

In conjunction with Equation 7 we may use another diffusion relationship which gives the coefficient at any temperature in terms of the coefficient at infinite temperature.

$$D = D_o e^{-\Delta H/RT} \tag{8}$$

Where D_o = diffusion coefficient at infinite temperature (cm^2/sec)

ΔH = activation energy for the process (cal/mol)

R = universal gas constant (=1.986 cal/^oC/mol)

T = absolute temperature (degrees Kelvin)

Substituting from Equation 8 into Equation 7 we get:

$$t^{-1} = \frac{2D}{x^2} = 2 D_o x^{-2} e^{-\Delta H/RT} \tag{9}$$

$$\text{or } \log_{10} t^{-1} = \log_{10} (2D_o x^{-2}) - \frac{\Delta H}{RT} \log_{10} e \tag{10}$$

and for a particular x, ΔH and D_o:

$$\log_{10} t^{-1} = C_1 - \frac{C_2}{T} \tag{11}$$

Where C_1 and C_2 are constants. It follows that a plot of $\log_{10} t^{-1}$ against $1/T$ should be a straight line.

For evaluation of Equation 10 the following values of the constants due to Wert[29] have been used:

For carbon in α- iron $\Delta H = 20,100$ cal/mol. $D_o = 0.02$ cm^2/sec

For nitrogen in α- iron $\Delta H = 18,200$ cal/mol. $D_o = 0.003$ cm^2/sec

The value of $x = 2 \times 10^{-8}$ cm. has been retained and when these figures are substituted in Equation 10 we obtain,

$$\text{For carbon,} \quad \log_{10} t^{-1} = 10.00 - \frac{4,400}{T} \tag{12}$$

$$\text{For nitrogen} \quad \log_{10} t^{-1} = 9.18 - \frac{4000}{T} \tag{13}$$

These equations are plotted as Curves II and III in Fig. 18 with $\log_{10} t^{-1}$ as ordinate and 1000/T as abscissa. For comparison, Muir's experimental results, as interpreted by Nabarro,[27] are shown in the same figure and these constitute Curve I.

It is seen that the three lines in Fig. 18 lay close together in the range of temperature examined and that the shorter the time, the higher the temperature must be for effective aging to occur. This underlines the point previously mentioned that at higher speeds of stressing, greater mobility of the interstitial atoms is required to re-anchor dislocations which, in turn, means a higher temperature is required.

If we now apply Fig. 18 to conditions of repeated load and assume, as previously stated, that the time t available for aging is the time of one loading cycle then, from Curves II and III, the corresponding value of 1000/T may be read off. This value of T will be the temperature at which the material should have a maximum life at the specified loading frequency for stresses above the endurance limit.

In the present experiments the machine speed was 2,600 r. p. m. which represents a cyclic time of 60/2600 seconds. The value of $\log_{10} t^{-1}$ is then 1.637 and, from Fig. 18, the corresponding value of 1000/T is 1.89 for both carbon and nitrogen. This gives a value of T of 530°K or 500°F, the temperature at which low carbon steel should exhibit a maximum fatigue strength when the cyclic rate is 2,600 per minute.

In order to establish possible upper and lower bounds for the predicted peaking temperature, the effects of varying the assumed values of ΔH, $\underline{x}$ and $\underline{t}$ are shown in Figs. 19 and 20. These figures are of the same type as Fig. 18. They show essentially the time taken, at different temperatures, for carbon and nitrogen atoms to travel the indicated distances with different values of ΔH.

In Fig. 19 values of ΔH have been selected which vary approximately $\pm$ 20% from the nominal values of 20,100 and 18,200 cal/mol. for carbon and nitrogen respectively. For comparison, the carbon line from Fig. 18 has been replotted in Figs. 19 and 20. The horizontal lines in these figures represent the values of $\log_{10} t^{-1}$ for values of $\underline{t}$ corresponding to different numbers of revolutions. The intersection of these horizontals with the various plotted lines give predicted peaking temperatures for the different conditions. For example, if the time available for aging is, in reality, half a revolution and the effective value of ΔH for nitrogen is 23,000 cal/mol., then from Fig. 19 a peak in fatigue life would be expected at a value of T given by $\frac{1000}{T} = 1.54$ i. e., T = 700°F. This would be the upper limit of predicted temperature within the conditions prescribed for the construction of the figure.

The lower limit for nitrogen is given by, say, allowing 100 revolutions for aging to occur with an effective ΔH of 13,000 cal/mol.

The corresponding value of $\frac{1000}{T}$ is 3.52 giving T = 50°F. The predicted range therefore has the limits 50° to 700°F. In fact it is doubtful whether ΔH for nitrogen could differ much from 18,200 cal/mol. since this quantity has often been reliably measured. However, the concept of the strain aging process which is being proposed is essentially concerned with the state of affairs in a highly worked region and there are grounds for believing that the value of ΔH might, in such circumstances, deviate somewhat from the value operative in an annealed region.

In Fig. 20 values of $\underline{x}$ which differ by an order of magnitude from the nominal 2×10^{-6} cm. have been used to illustrate the effect on peaking temperature obtained by varying the distance the interstitial atoms have to move. Using a similar method of analysis to that employed in the previous figure, the lower bound of peaking temperature is found to be 130°F corresponding to an aging time of 100 revolutions with a distance $\underline{x}$ of 10^{-7} cm. The upper bound is found to be 750°F for an aging time of half a revolution with a distance $\underline{x}$ of 10^{-5} cm.

As in the case of ΔH, very wide variations have been allowed here for the linear dimension $\underline{x}$ of the pattern. A distance of 10^{-7} cm. is only a few atomic distances and it seems doubtful whether the necessary precipitation of interstitials could take place wholly from such a very small domain. At the other extreme, a distance of 10^{-5} cm. would involve diffusion from the interslip region.

The limits of the predicted peaking temperature are thus 50° - 750°F, not a large range considering the generous variations allowed for ΔH, $\underline{t}$ and $\underline{x}$. The value of 500°F, calculated from the nominal values, falls near the center of the range.

(b) Cottrell's Strain Aging Theory

The analysis based on Nabarro's method assumes that the interstitial atoms have to move a certain distance, namely 2×10^{-6} cm., in order to achieve pinning. The theory does not consider the exact paths travelled by the atoms nor does it predict the number of atoms, or the fraction of the total solute, arriving at dislocations in a given time at a given temperature.

Later work by Cottrell, based on his own model which has been described, provides such information and may be used as a somewhat different approach to estimate the temperature at which maximum fatigue life may be expected.

It has been shown by Cottrell[25] that the binding energy between a solute atom and a dislocation is given by:

$$U = \frac{4}{3} G e r_a^3 b \frac{1+\nu}{1-\nu} \frac{\sin\theta}{R} \qquad (14)$$

Where U = Binding energy (usually expressed in eV units.

1 eV = 1.592×10^{-12} erg)

G = Rigidity Modulus

ν = Poissons Ratio

b = Slip distance (cms.) associated with the passage of a dislocation.

r_a and $r_a(1 + e)$ are the atomic radii (in cms.) of the solvent and solute atoms.

R and θ are the polar co-ordinates of the position of the solute atom with the dislocation at the origin. (See Fig. 21)

Equation 14 may be written :

$$U = A \frac{\sin\theta}{R} \qquad (15)$$

Where A depends on the elastic constants, the volume change caused by the solute atom and the strength of the dislocation. For carbon and nitrogen

in body-centered iron the value of A is about 3×10^{-20} dyne cm.^{2} Equation 15 breaks down at the center of the dislocation where linear elasticity theory is not applicable, but a generalized equation will be introduced later to overcome this difficulty. It follows from Equation 15 that U is constant when $\frac{\text{Sin } \theta}{R}$ is constant, which means that equipotential lines (i. e. lines of constant U) are circles passing through the center of the dislocation and centered on the y axis. This may be shown by reference to Fig. 21 in which the circle having its center at C has a radius equal to 'a'. In this circle $\frac{\text{Sin } \theta}{R} = 2a = \text{constant}$.

The remainder of the theory is developed by Cottrell and Bilby[30] and by Cottrell.[31] The line of reasoning is that the change in U from one circle to the next provides a force F on each solute atom which gives to it a drift velocity $\underline{v}$, in a direction perpendicular to the equipotential line, given by:

$$v = (D/kT)\ F \qquad (16)$$

Where k = Boltzmann's Constant = 1.38×10^{-16} erg/deg.

Motion of the solute atoms will therefore take place along the set of orthogonal circles $\frac{\text{Cos } \theta}{R}$ until they reach the position of maximum binding, the point situated just below the dislocation at $\theta = \frac{3\pi}{2}$. From Equation 15 and 16 it is possible to show that the number of solute atoms which will arrive at the dislocation in time $\underline{t}$ is given by:

$$N_t = 3n_o\rho \left[\frac{\pi}{2}\right]^{1/3} \left[\frac{ADt}{kT}\right]^{2/3} \qquad (17)$$

Where N_t = Number of solute atoms arriving at dislocations per unit volume of material in time $\underline{t}$.

n_o = Total number of atoms in solution per unit volume.

ρ = Dislocation density (number per unit area).

D = Diffusion coefficient at absolute temperature T.

The fraction f of the original solute which segregates in time t is then:

$$f = \alpha \rho \left[\frac{ADt}{kT}\right]^{2/3} \qquad (18)$$

Where α is a number nearly equal to 3.

Equation 18 is not applicable to the later stages of aging but Harper[32] has modified it to Equation 19 which is valid throughout aging.

$$f = 1 - \exp. \left[-\alpha \rho \frac{ADt}{kT}\right]^{2/3} \qquad (19)$$

The linear relationship between log (1-f) and $t^{2/3}$ has been confirmed experimentally by Harper for temperatures up to about 50°C. There seems to be no reason why the relationship should not be valid for somewhat higher temperatures.

Turning attention once more to conditions of repeated loading, the problem is to determine at what temperature sufficient solute atoms can segregate to dislocations to pin them in the time available for aging. We have the following data to work with,

(i) The solubility (weight percent) of carbon and nitrogen in α- iron for a wide range of temperature. See Dijkstra.[33]

(ii) The weight percent of carbon or nitrogen necessary to pin 10^{12} dislocations per sq. cm. Cottrell and Churchman[26] showed that this is between 10^{-3} and 10^{-2} weight percent.

(iii) Equation 19.

(iv) The assumption that the time available for aging is of the order of the time for one loading cycle

The speed of the machine in the present experiments was 2,600 r. p. m. Hence a computation was made of the minimum temperature at which 10^{-3} to 10^{-2} weight percent of carbon or nitrogen can segregate in $\frac{60}{2600}$ seconds.

The procedure employed was to plot, for each interstitial, a curve of solubility against temperature and also a curve, computed from Equation 19, of the fraction, f, segregating at different temperatures during a time of $\frac{60}{2600}$ seconds. The product of these two curves gave a curve of the actual weight percent segregating in the cyclic time. From this last curve the temperatures were determined corresponding to segregated weight percents of 10^{-2} and 10^{-3}. These temperatures represented upper and lower bounds to achieve effective aging in the cyclic time.

In evaluating Equation 19 the following values were used:

$\alpha = 3$

$\rho = 10^{12}$ dislocations/sq. cm.

$A = 3 \times 10^{-20}$ dynes cm.^{2}

$k = 1.38 \times 10^{-16}$ erg/deg.

As in the previous section dealing with Nabarro's work, values given by Wert[29] for the diffusion coefficients were employed, i. e.,

for carbon $D = 0.02\, e^{-20,100/RT}$

for nitrogen $D = 0.003\, e^{-18,200/RT}$

Corresponding values for T and f for carbon and nitrogen, as calculated from Equation 19, are shown in Tables V and VI respectively and then plotted as Curve II and Figs. 22 and 23 respectively. Curve I in these figures represents Dijkstra's[33] results for solubility and, as explained above. Curve III in both cases is the product of Curves I and II.

In Curve III of Fig. 22 the temperatures corresponding to segregated weight percents of 10^{-3} and 10^{-2} of carbon are 640 and 875°K respectively. These temperatures correspond to 685 and 1, 115°F.

In Curve III of Fig. 23 the temperatures corresponding to segregated weight percents of 10^{-3} and 10^{-2} of nitrogen are 467 and 575°K respectively. These temperatures correspond to 380 and 575°F.

It follows that, according to this procedure, peak life should occur in the range 685° to 1, 115°F for iron containing carbon and in the range 380° to 575°F for iron containing nitrogen. If both carbon and nitrogen are present a peak in the life vs. temperatures curve would be expected in both ranges of temperature unless there is some type of interaction between the two kinds of interstitial atoms.

To summarize the theoretical findings, both procedures indicate that a peak in the fatigue life, due to strain aging, should occur in the region of 500°F when the cyclic rate is 2, 600 r. p. m. A curve, calculated from Equation 10, giving the predicted temperatures for maximum fatigue strength for a range of cyclic rates of loading, is shown in Fig. 24.

BIBLIOGRAPHY

1 C. A. Edwards, D. L Phillips, Y. H. Liu, "The Yield Point in Steel," Journal Iron and Steel Inst., Vol CXLVII, No 1, p. 145p, (1943).

2. J. R. Low, Jr., and M. Gensamer, "Aging and Yield Point in Steel," Tr. Am. Inst. Min. Met. Eng., Vol. 158, pp. 207-249, (1944)

3. G. M. Sinclair, "An Investigation of the Coaxing Effect in Fatigue of Metals," Proc. A. S. T. M., Vol. 52, p. 743, (1952).

4. H. T. Corten, T. Dimoff, T. J. Dolan, M. Sugi, "An Appraisal of the Prot Method of Fatigue Testing" Part II. Technical Report under Navy Contract N6-ori-071 (04), Project NR-031-005, University of Illinois, June 1953.

5. H. F. Moore and N. J. Alleman, Progress Report on Tests of Low Carbon Steel at Elevated Temperatures, Proc. A. S. T. M. Vol. 31, p. 114, (1931).

6. W. L. Collins and J. O. Smith, "Fatigue and Static Load Tests of a High Strength Cast Iron at Elevated Temperatures," Proc. A. S. T. M. Vol. 41, p. 797, (1941).

7. G. M. Sinclair and T. J. Dolan, "Effect of Stress Amplitude on Statistical Variability of Fatigue Life of 75S-T6 Aluminum Alloy," Transactions Am. Soc. Mechanical Engrs., Vol. 75, p. 867, (1953).

8. K. A. Brownlee, "Industrial Experimentation," Chemical Publishing Co. Inc., Brooklyn, N. Y., (1947).

9. H. J. Gough and W. A. Wood, Proc. Roy. Soc. of London, Series A, Vol. 154, p. 510, (1936)

10. H. W. Paxton, M. A. Adams, T. B. Massalski, Phil. Mag., Vol. 43, No. 337, p. 257, (Feb. 1952).

11. C. Wert, "Precipitation out of Dual Solid Solutions of C and N_2 in α - Iron," Scientific Paper No. 1773, Westinghouse Research Labs., East Pittsburgh, Pa.

12. J. D. Fast, "Strain Aging in Iron and Steel," Philips Techn. Rev. Vol. 14, No. 2, p. 60, (1952).

13. F. Bolenrath and H. Cornelius, "Effect of Rest Periods on the Time and Fatigue Strengths of Metallic Materials," VDI-Z, Vol. 84, No. 18, (1940) (Translation No. 104, David Taylor Model Basin, 1942).

14 R. D. Heidenreich and W. Shockley, "Study of Slip in Aluminum Crystals by Electron Microscope and Electron Diffraction Methods," Report of a Conference on the Strength of Solids, Bristol (1947), (London: The Physical Soc.).

15. A. F. Brown, "Surface Effects in Plastic Deformation of Metals," Advances in Physics, (Phil. Mag. Supp.) Vol. 1, No. 4, p. 427, (Oct. 1952).

16. A. F. Brown and R. W. K. Honeycombe, "Microslip in Metal Crystals," Phil. Mag. Vol. 42, p. 1146, (Oct. 1951).

17. F. C. Frank and W. T. Read, Phys. Rev., Vol. 79, p. 722, (1950),

18. W. T. Read, Jr., "Dislocations in Crystals," McGraw Hill Book Co., Inc., (1953).

19. F. Seitz, "On the Generation of Vacancies by Moving Dislocations," Advances in Physics, (Phil. Mag. Supp.) Vol. I, No. 1, p. 1, (Jan. 1952).

20. A. H. Cottrell, "Theory of Dislocations" in "Progress in Metal Physics," (Ed. B. Chalmers) Vol. IV, (1952), London: Butterworth.

21. A. F. Brown, Journal Inst. of Metals, Vol. 80, p. 115, (1951-2).

22. R. O. Griffis, R. L. Kenyon, R. S. Burns, "The Aging of Mild Steel Sheets," Yearbook Am. Iron and Steel Inst., Vol. 23, pp. 142-165, (1933).

23. H. Quinney, "Further Tests on the Effect of Time in Testing," The Engineer, Vol. 161, pp. 669-673, (1936).

24. A. Nadai and M. J. Manjoine, "High Speed Tension Tests at Elevated Temperatures," J. Applied Mechanics, Vol. 63, pp. 77-91, (1941).

25. A. H. Cottrell, "Effect of Solute Atoms on the Behavior of Dislocations," as (14).

26. A. H. Cottrell and A. T. Churchman, J. Iron & Steel Inst., Vol. 162, p. 271, (1949).

27. F. R. N. Nabarro, "Mechanical Effects of Carbon in Iron," as (14).

28. J. Muir, "On the Recovery of Iron from Overstrain," Phil. Trans. Roy. Soc. of London. Series A, Vol 193, pt. I, (1900).

29. C. A. Wert, Phys. Rev., Vol. 79, pp. 601-605, (1950).

30. A. H. Cottrell and B. A. Bilby, Proc. Phys. Soc., A., Vol. 62, Pt. I., p. 49, (1949).

31. A. H. Cottrell, "Dislocations and Plastic Flow in Crystals," Chap. IV, Clarendon Press, Oxford, 1953.

32. S, Harper, Phys. Rev., Vol. 83, p. 709, (1951).

33. L. J. Dijkstra, Tr. Am. Inst. Min. and Met. Engrs., Vol. 185, pp. 252-260, (1949).

TABLE I

VALUES OF STUDENT'S "t"

See Brownlee [8]

Degrees of Freedom	Values of "t" for the following levels of significance.				
	0.10	0.05	0.02	0.01	0.001
4	2.13	2.78	3.75	4.60	8.61
9	1.83	2.26	2.82	3.25	4.78
18	1.73	2.10	2.55	2.88	3.92
∞	1.65	1.96	2.33	2.58	3.29

TABLE II

FATIGUE TEST RESULTS

N = No. of Cycles to Failure n = No. of Specimens in Sample

$$X = \Sigma(\log N)^2 - \frac{(\Sigma \log N)^2}{n}$$

	Cycles to Fracture 'N'	log N	$(\log N)^2$	
Batch I (Original Material) Tested at Room Temperature	54,500	4.73640	22.4335	
	54,700	4.73799	22.4486	
	59,500	4.77452	22.7960	n = 10
	76,400	4.88309	23.8446	Mean (log N) = 4.8911
	76,400	4.88309	23.8446	$\frac{(\Sigma \log N)^2}{n}$ = 239.2307
	78,200	4.89321	23.9435	X = 239.3619 - 239.2307
	83,200	4.92012	24.2076	= 0.1312
	87,900	4.94399	24.4430	
	107,800	5.03262	25.3273	
	127,700	5.10619	26.0732	
Σ	806,300	48.91122	239.3619	
Tested at 220° F.	109,800	5.04060	25.4076	
	114,900	5.06032	25.6068	
	115,200	5.06145	25.6183	n = 10
	121,900	5.08600	25.8674	Mean (log N) = 5.1205
	135,700	5.13258	26.3434	$\frac{(\Sigma \log N)^2}{n}$ = 262.1989
	138,600	5.14176	26.4377	X = 262.2490 - 262.1989
	141,900	5.15198	26.5429	= 0.0501
	147,100	5.16761	26.7042	
	150,200	5.17667	26.7980	
	153,600	5.18639	26.8986	
Σ	1,328,900	51.20536	262.2490	
Tested at 300° F.	43,900	4.64246	21.5524	
	75,800	4.87967	23.8112	
	117,600	5.07041	25.7091	n = 10
	131,200	5.11793	26.1932	Mean (log N) = 5.2281
	132,800	5.12320	26.2472	$\frac{(\Sigma \log N)^2}{n}$ = 273.3301
	158,900	5.20112	27.0516	X = 274.4357 - 273.3301
	217,100	5.33666	28.4799	= 1.1056
	257,300	5.41044	29.2729	
	508,900	5.70663	32.5656	
	620,100	5.79246	33.5526	
Σ	2,263,600	52.28098	274.4357	

TABLE II (Continued)

FATIGUE TEST RESULTS

	Cycles to Fracture 'N'	log N	$(\log N)^2$	
Batch I (Original Material) Tested at 420° F.	201,600 249,600 376,500 483,000 659,400 858,400 865,200 2,099,500 3,500,000* 3,585,000*	5.30449 5.39724 5.57576 5.68395 5.81915 5.93369 5.93712 6.32211 6.54407 6.55449	28.1376 29.1302 31.0891 32.3073 33.8625 35.2087 35.2494 39.9691 42.8248 42.9613	* Denotes specimen did not break. n = 10 Mean (log N) = 5.9072 $\frac{(\Sigma \log N)^2}{n} = 348.9509$ X = 350.7400 - 348.9509 = 1.7891
Σ	12,878,200	59.07207	350.7400	
Tested at 530° F.	87,800 142,500 154,200 158,800 172,400 177,600 181,200 198,900 257,400 289,800	4.94349 5.15381 5.18808 5.20085 5.23654 5.24944 5.25816 5.29863 5.41061 5.46210	24.4381 26.5618 29.9162 27.0488 27.4214 27.5566 27.6482 28.0755 29.2747 29.8345	n = 10 Mean (log N) = 5.2407 $\frac{(\Sigma \log N)^2}{n} = 274.5939$ X = 277.7758 - 274.5939 = 3.1819
Σ	1,820,600	52.40171	277.7758	
Tested at 700° F.	24,500 24,800 25,600 32,200 32,700 33,200 42,600 56,100 70,100 72,900	4.38917 4.39445 4.40824 4.50786 4.51455 4.52114 4.62941 4.74896 4.84572 4.86273	19.2648 19.3112 19.4326 20.3208 20.3812 20.4407 21.4314 22.5526 23.4810 23.6461	n = 10 Mean (log N) = 4.5822 $\frac{(\Sigma \log N)^2}{n} = 209.9677$ X = 210.2624 - 209.9677 = 0.2947
Σ	414,700	45.82223	210.2624	

TABLE II (Continued)

FATIGUE TEST RESULTS

	Cycles to Fracture 'N'	log N	$(\log N)^2$	
Batch II (Carbon and Nitrogen Removed) Tested at Room Temperature	63,900 83,800 85,600 88,100 92,800 107,300 115,300 115,900 126,700 136,500	4.80550 4.92324 4.93247 4.94498 4.96755 5.03060 5.06183 5.06408 5.10278 5.13513	23.0928 24.2383 24.3293 24.4528 24.6766 25.3069 25.6221 25.6449 26.0384 26.3696	n = 10 Mean (log N) = 4.9968 $\frac{(\Sigma \log N)^2}{n} = 249.6817$ X = 249.7717 - 249.6817 = 0.0900
Σ	1,021,300	49.96816	249.7717	
Tested at 420° F.	152,900 170,000 171,000 180,700 199,100 200,200 253,500 326,800 333,000 600,800	5.18441 5.23045 5.23300 5.25696 5.29907 5.30146 5.40398 5.51428 5.52244 5.77873	26.8781 27.3576 27.3843 27.6356 28.0801 28.1055 29.2030 30.4073 30.4973 33.3937	n = 10 Mean (log N) = 5.3725 $\frac{(\Sigma \log N)^2}{n} = 288.6382$ X = 288.9425 - 288.6352 = 0.3073
Σ	2,588,000	53.72478	288.9425	

TABLE II (Concluded)

FATIGUE TEST RESULTS

	Cycles to Fracture 'N'	log N	$(\log N)^2$	
Batch III (Nitrogen Reintroduced) Tested at Room Temperature	56,200	4.74974	22.5600	
	59,900	4.77743	22.8238	
	62,700	4.79727	23.0138	n = 10
	70,600	4.84880	23.5109	
	81,000	4.90849	24.0933	Mean (log N) = 4.90431
	89,000	4.94939	24.4965	$\frac{(\Sigma \log N)^2}{n} = 240.5230$
	90,200	4.95521	24.5541	
	90,300	4.95569	24.5589	X = 240.6310 - 240.5230
	102,700	5.00945	25.0946	
	123,500	5.09167	25.9251	= 0.1080
Σ	825,600	49.04314	240.6310	
Tested at 300° F.	1,380,000*			* Denotes specimen did not break.
	3,242,900*			
	3,596,600*			n = 5
	3,654,800*			
	4,089,100*			
Tested at 420° F.	93,600	4.97128	24.7136	
	601,000	5.77887	33.3953	n = 5
	818,700	5.91312	34.9650	Mean (log N) = 5.81164
	1,011,600	6.00501	36.0601	$\frac{(\Sigma \log N)^2}{n} = 168.8759$
	2,454,300	6.38993	40.8312	
				X = 169.9652 - 168.8759
				= 1.0993
Σ	4,879,200	29.05821	169.9652	

TABLE III

MEAN VALUES OF FATIGUE LIFE AND 95% CONFIDENCE LIMITS

Batch & Temperature	log $\bar{N}$	$\bar{N}$ cycles	Standard Deviation σ	95% Confidence Limits (log $\bar{N} \pm \frac{t\sigma}{\sqrt{n}}$)			
				Upper		Lower	
				log N_u	N_u	log N_L	N_L
Batch I Room Temp.	4.89112	77,800	0.12067	4.97728	95,000	4.80496	63,800
Batch I 220° F.	5.12053	132,000	0.05477	5.15964	144,400	5.08142	120,600
Batch I 300° F.	5.22810	169,100	0.35050	5.47829	300,800	4.97791	95,000
Batch I 420° F.	5.90721	807,700	0.44586	6.22555	1,681,000	5.58887	388,100
Batch I 530° F.	5.24017	173,800	0.14217	5.34168	219,600	5.13866	137,600
Batch I 700° F.	4.58222	38,200	0.18097	4.66002	45,700	4.50442	32,000
Batch II Room Temp.	4.99682	99,300	0.09950	5.06786	116,900	4.92578	84,300
Batch II 420° F.	5.37248	235,700	0.18483	5.50445	319,500	5.24051	174,000
Batch III Room Temp.	4.90431	80,200	0.10954	4.98252	96,100	4.82610	67,000
Batch III 300° F.	---	---	---	----	---	---	---
Batch III 420° F.	5.81164	648,100	0.52187	6.46032	2,886,000	5.16296	145,500

N.B. The value of 't' for the 5% level is found from Table I according to the number of degrees of freedom (= n-1).

TABLE IV

COMPARISON BETWEEN SAMPLE MEANS

$$t = \frac{\log \bar{N}_1 - \log \bar{N}_2}{\lambda} \sqrt{\frac{n_1 n_2}{n_1 + n_2}} \qquad \lambda^2 = \frac{X_1 + X_2}{n_1 + n_2 - 2}$$

Comparison Between 1	and 2	$X_1 + X_2$	λ^2	λ	t	Level of Significant Difference
Batch I R.T.	Batch I 220°	0.1813	0.01007	0.100	5.13	
Batch I R.T.	Batch I 300°	1.2368	0.0687	0.262	2.98	
Batch I R.T.	Batch I 420°	1.9203	0.1067	0.327	6.95	
Batch I 420°	Batch I 220°	1.8392	0.1022	0.320	5.99	All
Batch I 420°	Batch I 300°	2.8947	0.1608	0.410	3.84	Less
Batch I 420°	Batch I 530°	4.9710	0.2984	0.546	2.73	Than
Batch I 420°	Batch I 700°	2.0838	0.1037	0.322	9.20	5%
Batch II R.T.	Batch I R.T.	0.2212	0.0112	0.106	2.28	
Batch II 420°	Batch I 420°	2.0964	0.1166	0.342	3.49	
Batch II R.T.	Batch II 420°	0.3973	0.0221	0.148	5.66	
Batch III R.T.	Batch I R.T.	0.2392	0.0122	0.111	0.27	> 10%

N.B. For relevant values of 't' see Table I with degrees of freedom (n_1+n_2-2).

TABLE V

FRACTION 'f' OF CARBON IN SOLUTION SEGREGATING TO DISLOCATIONS IN CYCLIC TIME

$$Z_c = 64.8 \times 10^6 \left[\left(e^{-10,400/T}\right)/T\right]^{2/3}$$

T deg.abs.	$\frac{10,400}{T}$	$\left(\frac{10,400}{T}\right)$	$\left[\frac{e^{(-10,400/T)}}{T}\right]^{2/3}$	Z_c	$f = 1 - e^{(-Z_c)}$
373	27.9	132×10^{10}	7.43×10^{-12}	482×10^{-6}	0
450	23.1	1075×10^{7}	34.8×10^{-10}	225×10^{-3}	0.202
473	22.0	335×10^{7}	73.5×10^{-10}	476×10^{-3}	0.380
500	20.8	1085×10^{6}	1.15×10^{-8}	97.5×10^{-2}	0.623
573	18.1	708×10^{5}	8.48×10^{-8}	55×10^{-1}	0.996
673	15.4	479×10^{4}	45.9×10^{-8}	29.8	1

TABLE VI

FRACTION 'f' OF NITROGEN IN SOLUTION SEGREGATING TO DISLOCATIONS IN CYCLIC TIME

$$Z_N = 18.2 \times 10^6 \left[\left(e^{-9,400/T}\right)/T\right]^{2/3}$$

T deg.abs.	$\frac{9,400}{T}$	$\left(\frac{9,400}{T}\right)$	$\left[\frac{e^{(-9,400/T)}}{T}\right]^{2/3}$	Z_N	$f = 1 - e^{(-Z_N)}$
293	32.1	8.7×10^{13}	11.55×10^{-12}	209×10^{-6}	0
373	25.2	8.75×10^{10}	9.42×10^{-10}	171×10^{-4}	0.020
450	20.8	10.85×10^{8}	1.61×10^{-8}	29.6×10^{-2}	0.258
473	19.9	4.38×10^{8}	2.86×10^{-8}	51.8×10^{-2}	0.404
500	18.8	146×10^{6}	5.73×10^{-8}	106×10^{-2}	0.654
573	16.4	13.2×10^{6}	25.9×10^{-8}	469×10^{-2}	0.992
673	14.0	12.1×10^{5}	1.15×10^{-6}	20.8	1

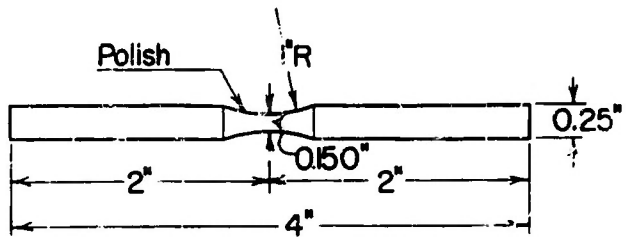

Fig.1 Rotating Beam Fatigue Specimen

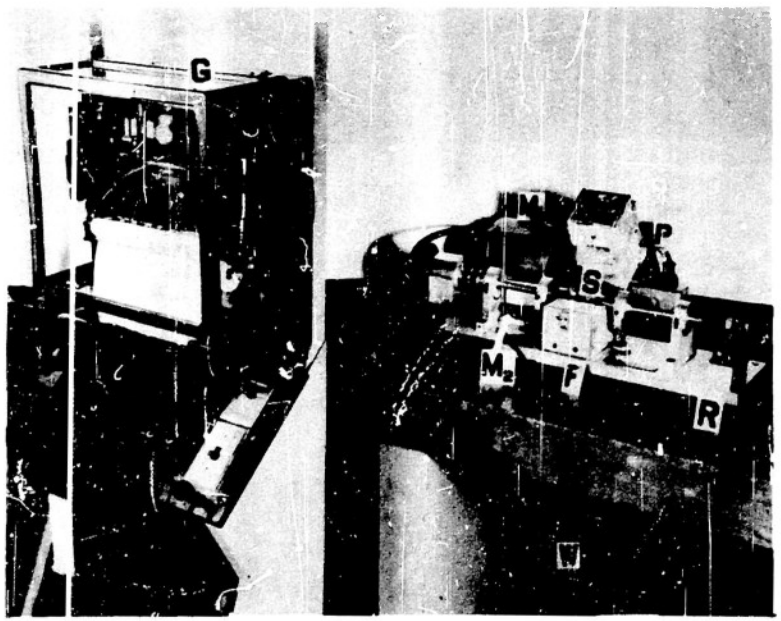

Fig. 2 Rotating Beam Fatigue Machine

F - Furnace
G - Temperature Controller
P - Mains Point
M_1 - Motor
M_2 - Microswitch
R - Revolution Counter
S - Specimen
W - Weight Hanger

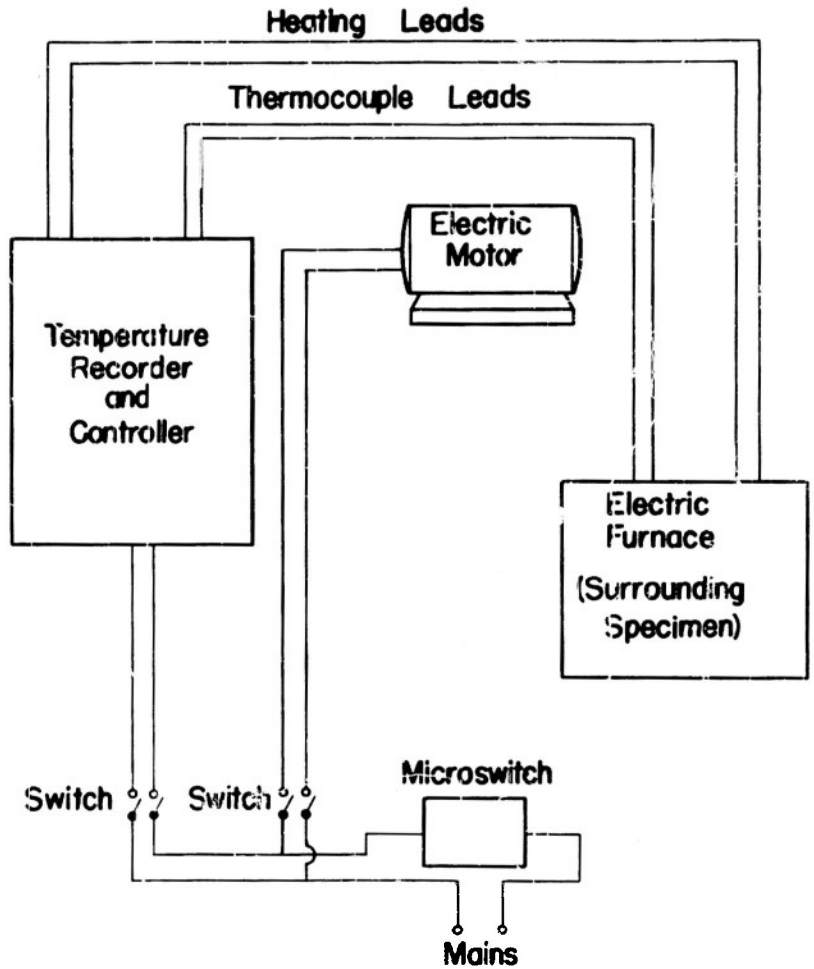

Fig. 3 Schematic Diagram of Electrical Connections

The motor drives the specimen through a belt and pulley arrangement. The microswitch automatically breaks the heating and motor circuits when the specimen falls.

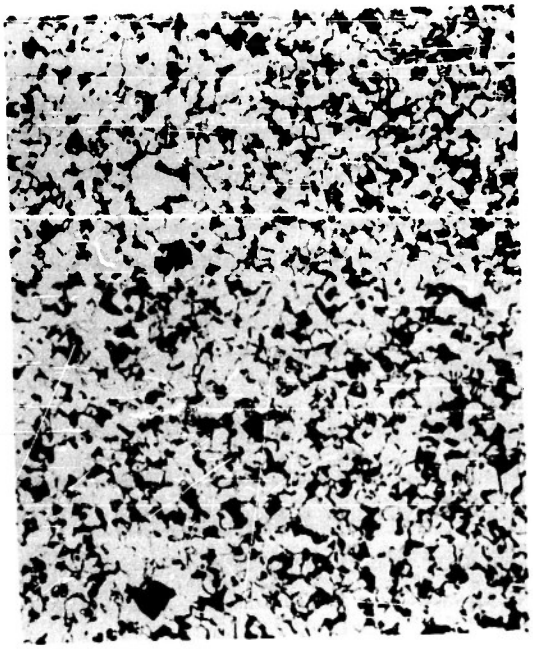

Fig 4 Material as Received (×150)

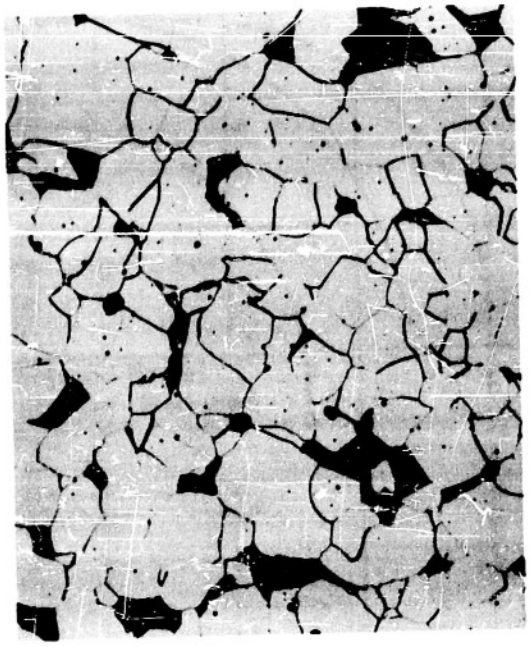

Fig.5 Helium Treated Batch I (×150)

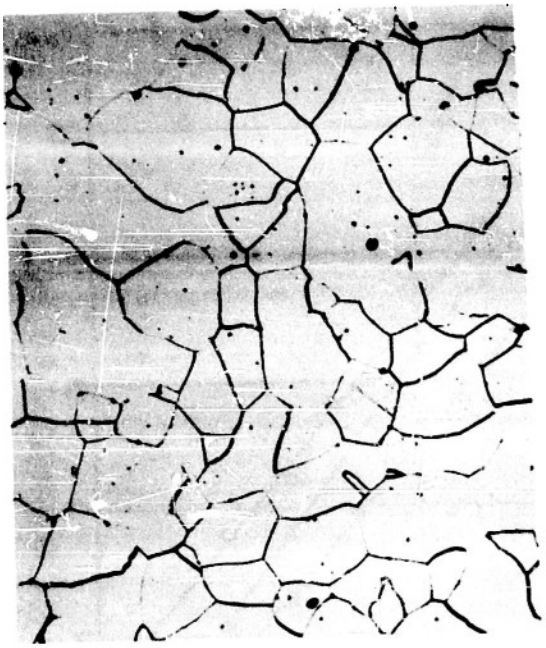

Fig.6 Wet Hydrogen Treated Batch II (×150)

Fig. 7 Wet Hydrogen Treated then Ammonia Treated Batch III (×150)

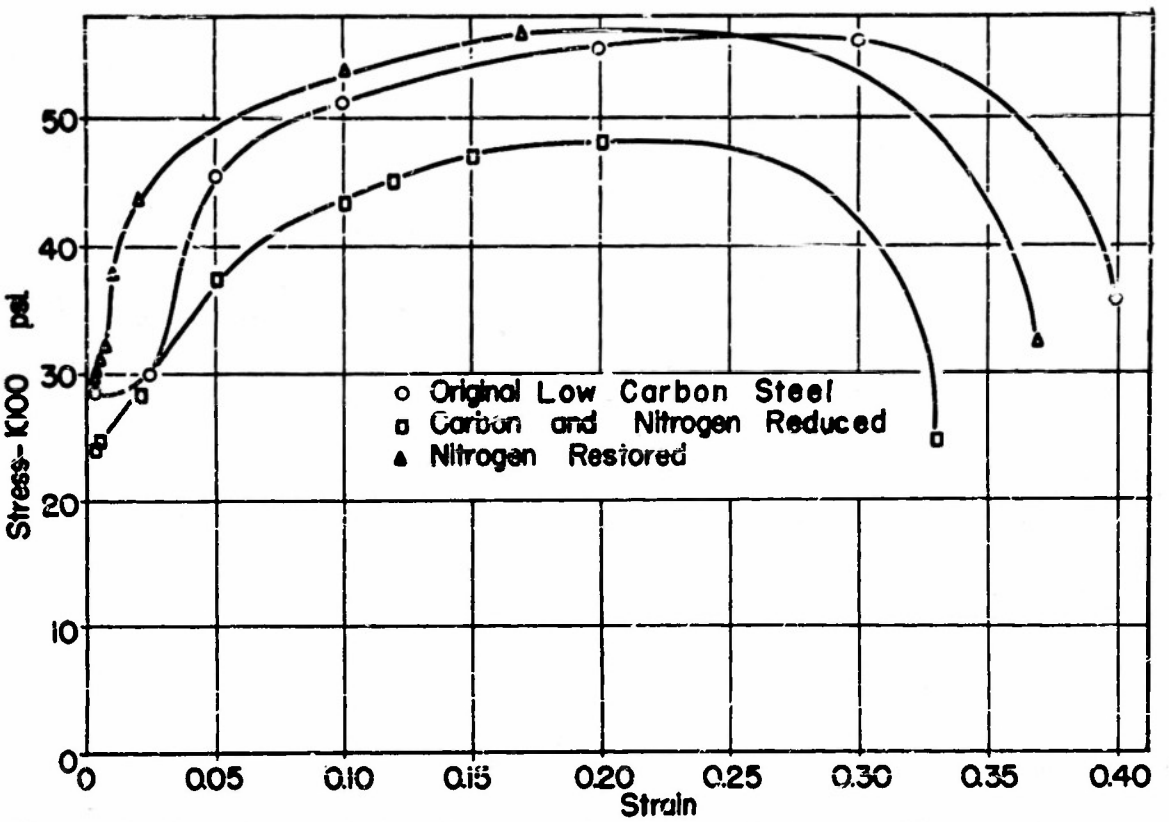

Fig. 8 Tensile Stress-Strain Curves After the Various Treatments

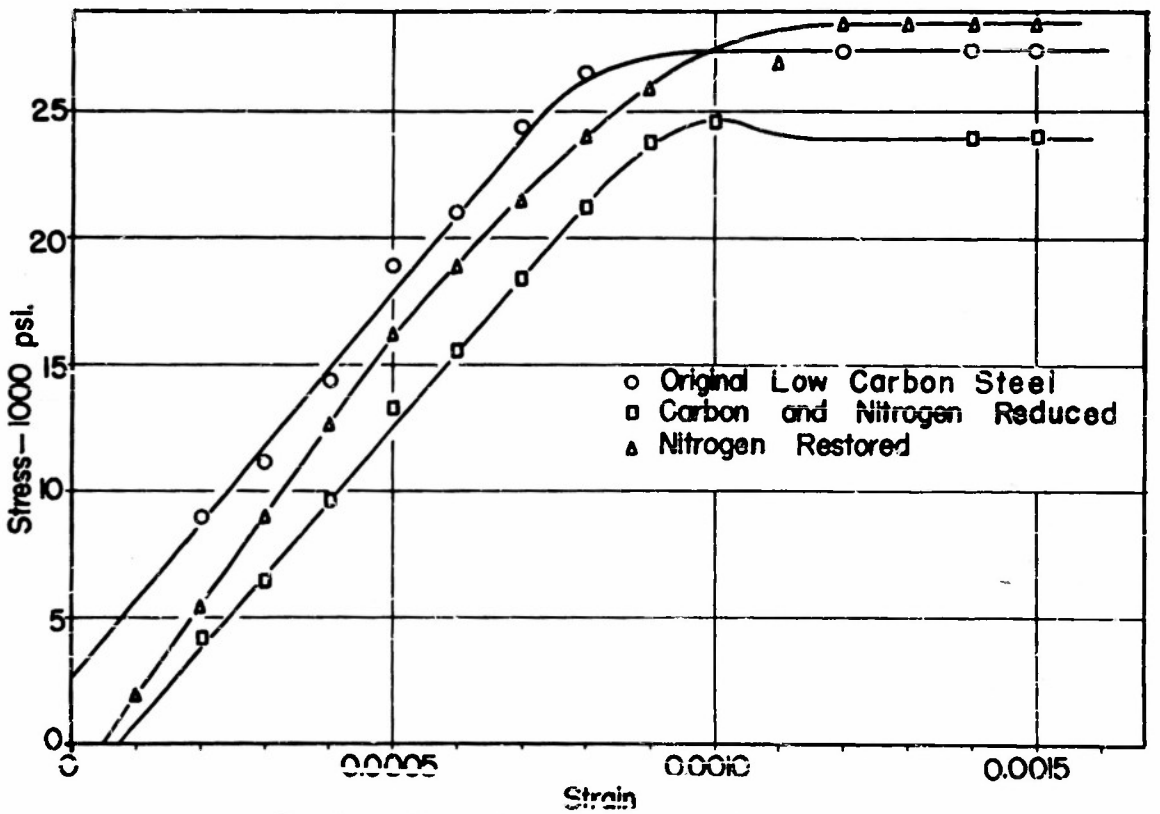

Fig 9 Tensile Stress-Strain Curves (Early Portions)

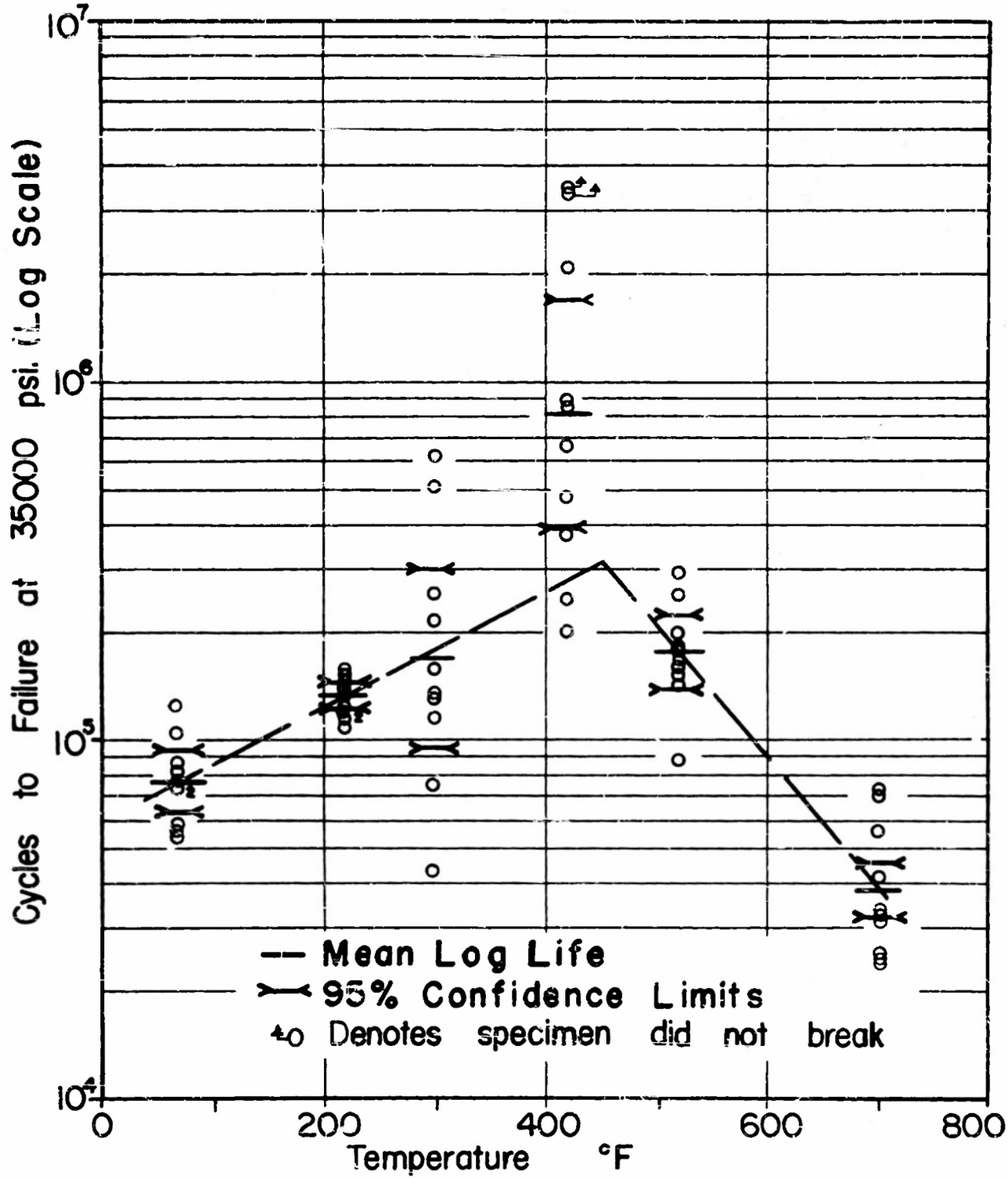

Fig. 10 Test Results for the Original Low Carbon Steel (Helium Treated)

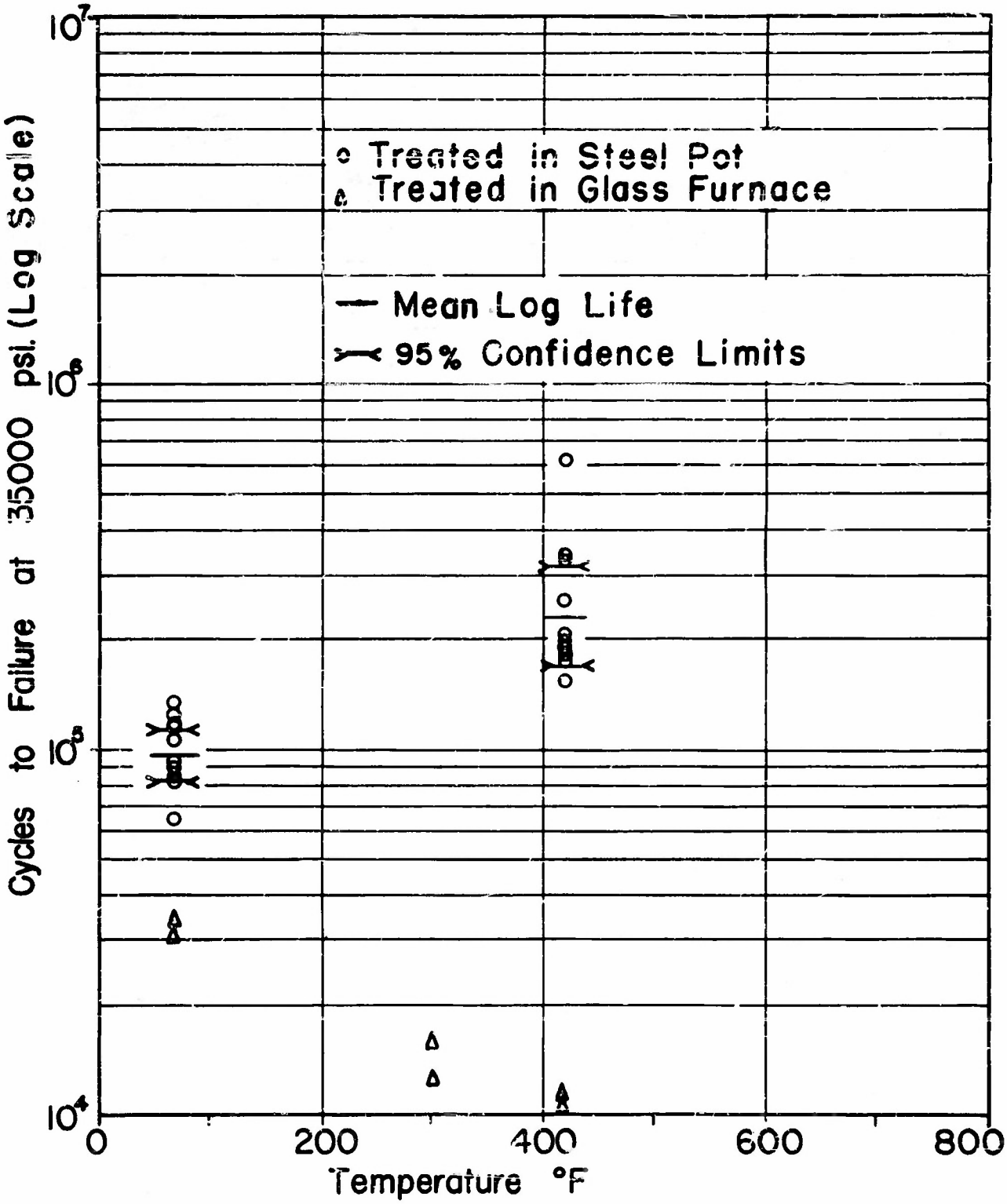

Fig.11 Test Results for Specimens with Carbon and Nitrogen Reduced (Wet Hydrogen Treated)

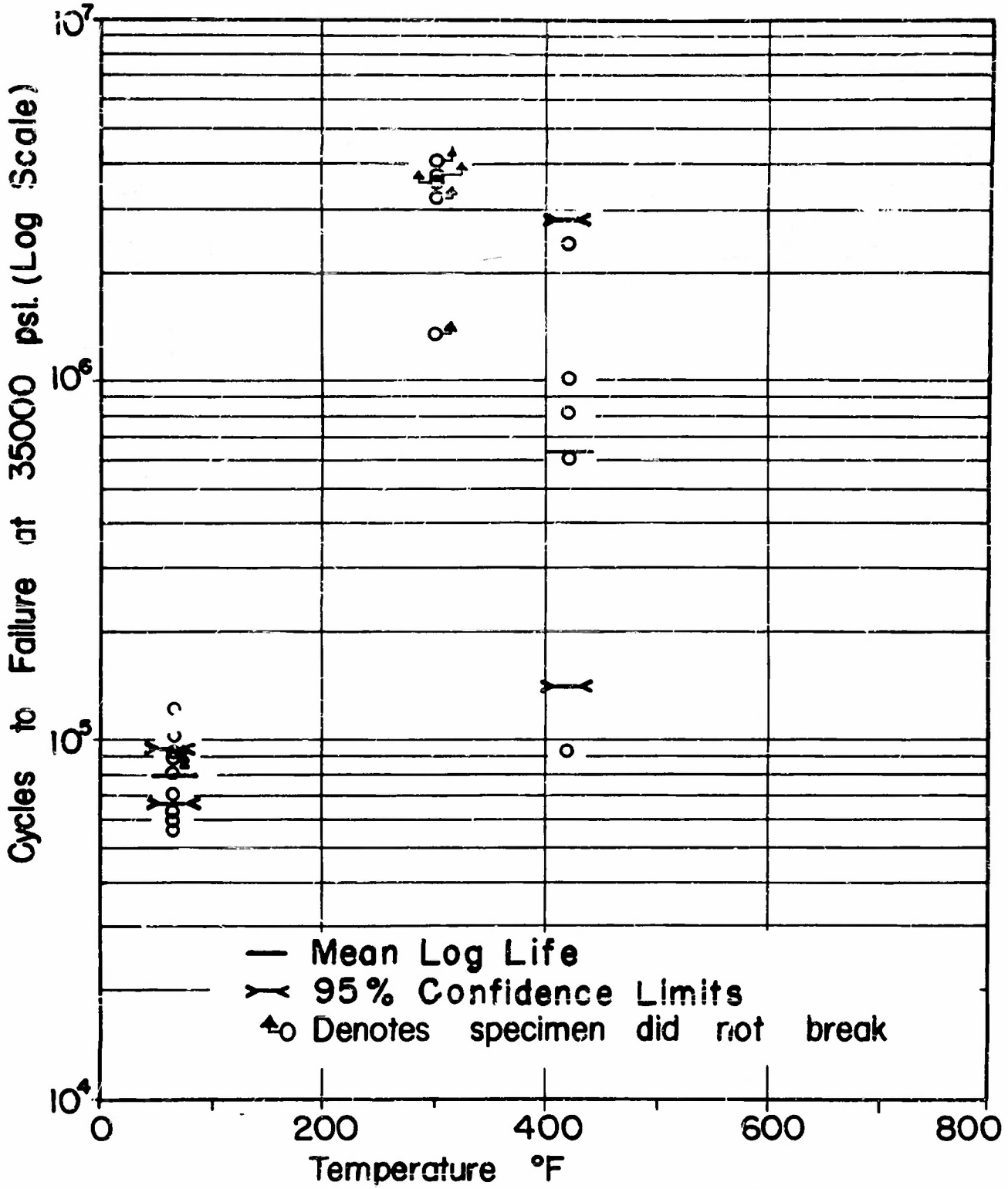

Fig.12 Test Results for Specimens with Nitrogen Restored (Wet Hydrogen Treated, then Ammonia Treated)

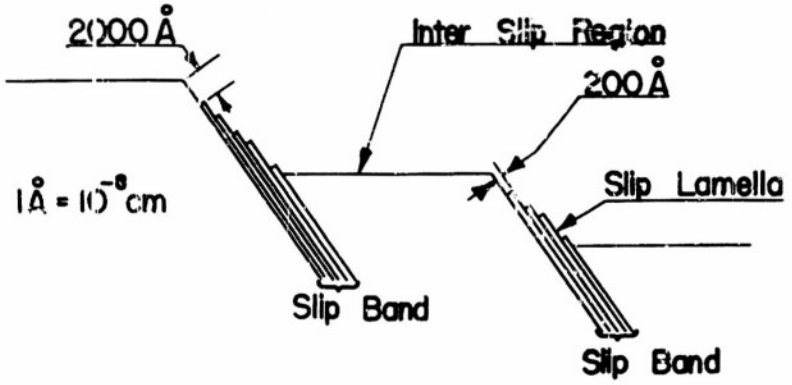

Fig.13 Structure of Slip Bands in Aluminum

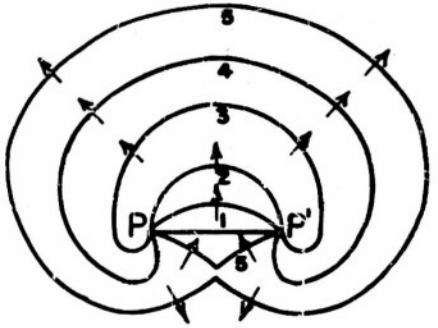

Fig.15 The Frank–Read Source

Under an applied force the dislocation moves into the successive positions 1-5. In this fashion many dislocation rings may be generated from a single dislocation.

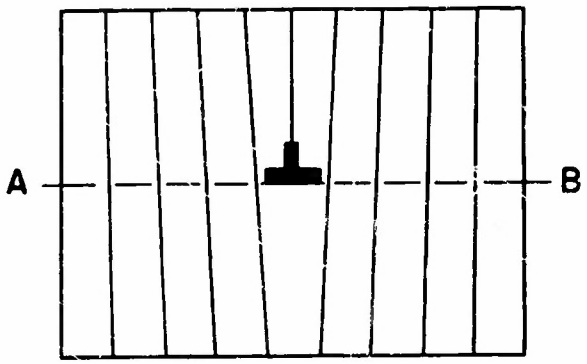

Fig.14 Schematic Representation of A Dislocation

The vertical lines are planes of atoms. The slip plane is AB.

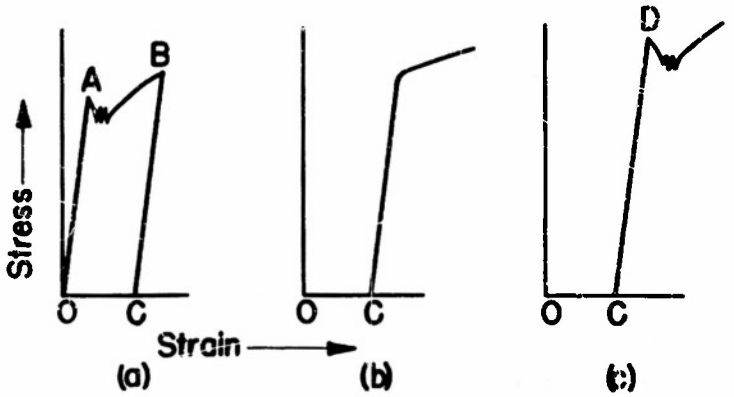

Fig.16 Strain Aging in Tension

(a) Originally strained to B and unloaded to C. An upper yield point occurs at A.

(b) Curve obtained if immediately reloaded. No upper yield point.

(c) Curve obtained if reloaded after resting. (at room or mildly elevated temperature). Upper yield point obtained at D.

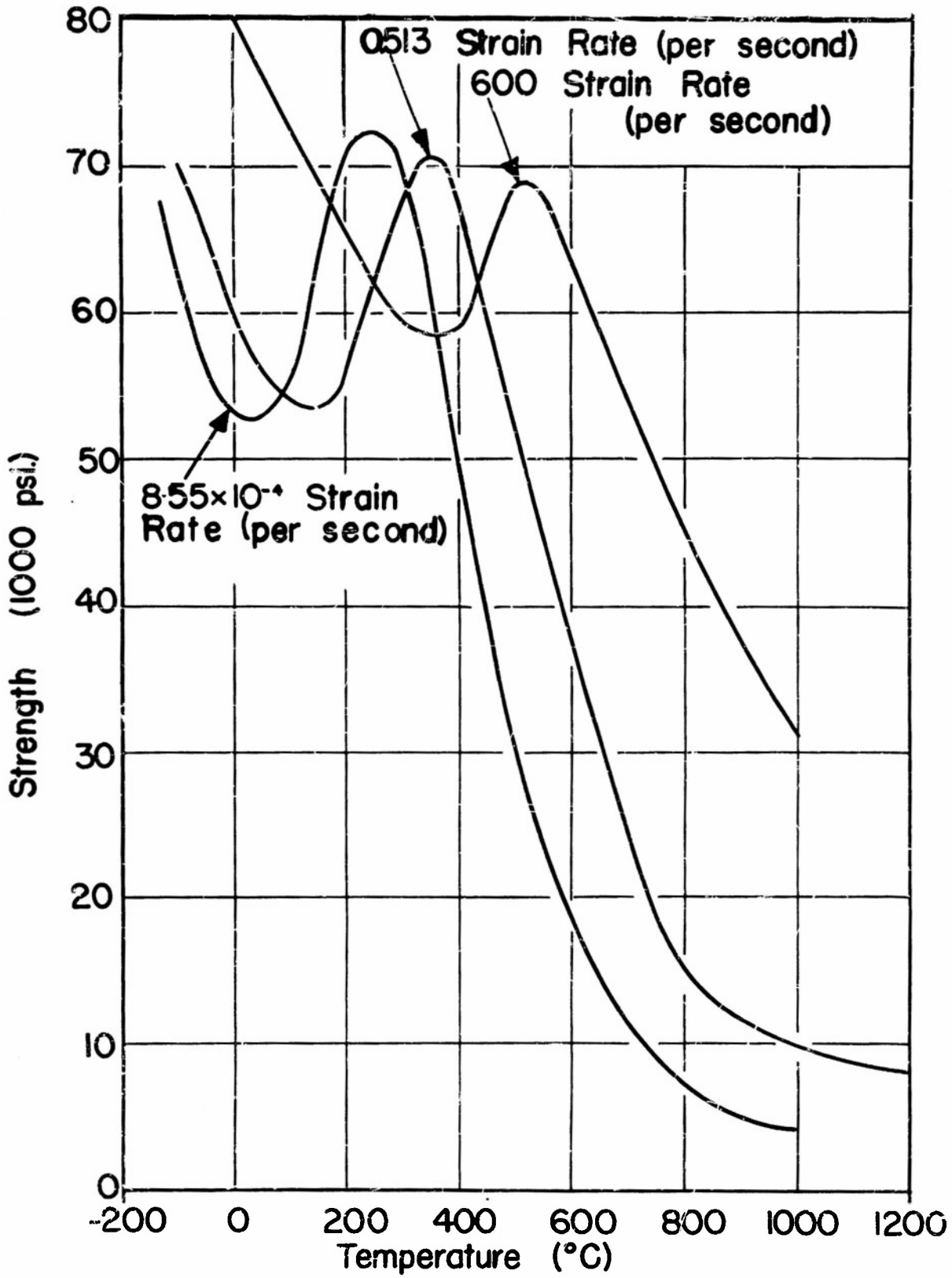

Fig. 17 Effect of Temperature and Strain Rate on the Tensile Strength of Steel.[24]

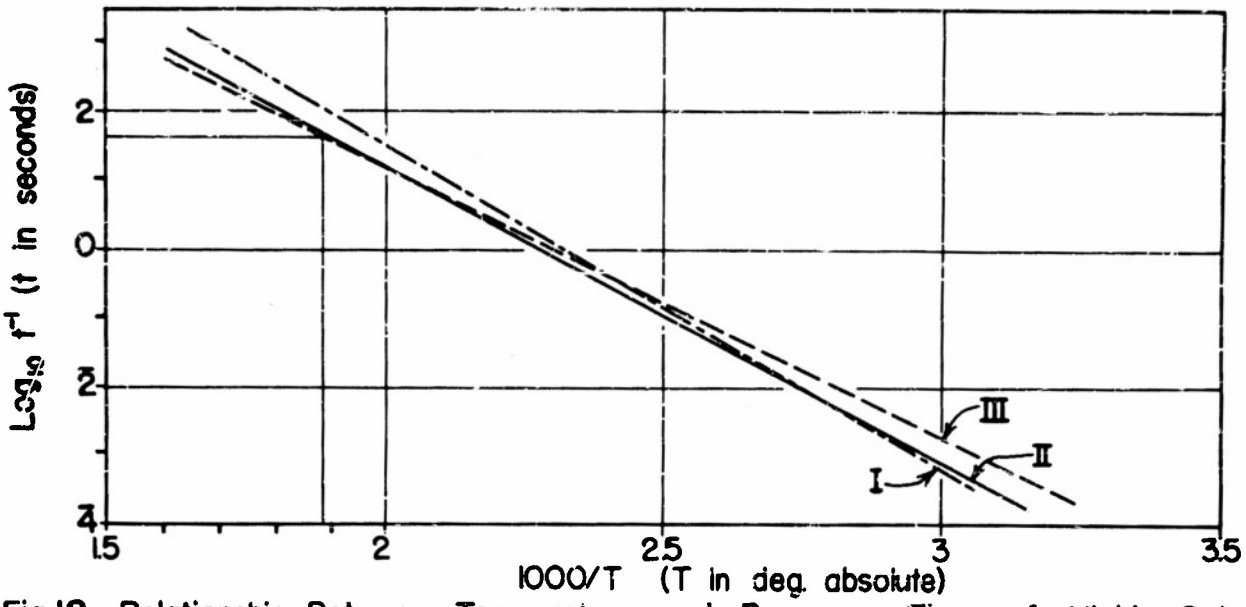

Fig.18 Relationship Between Temperature and Recovery Time of Yield Point in Low Carbon Steel

I Muir's Experimental Results for time of recovery of yield point in mild steel. (After Nabarro)

II Representing the time taken for carbon atoms to travel 2×10^{-6} cm.

III Representing the time taken for nitrogen atoms to travel 2×10^{-6} cm.

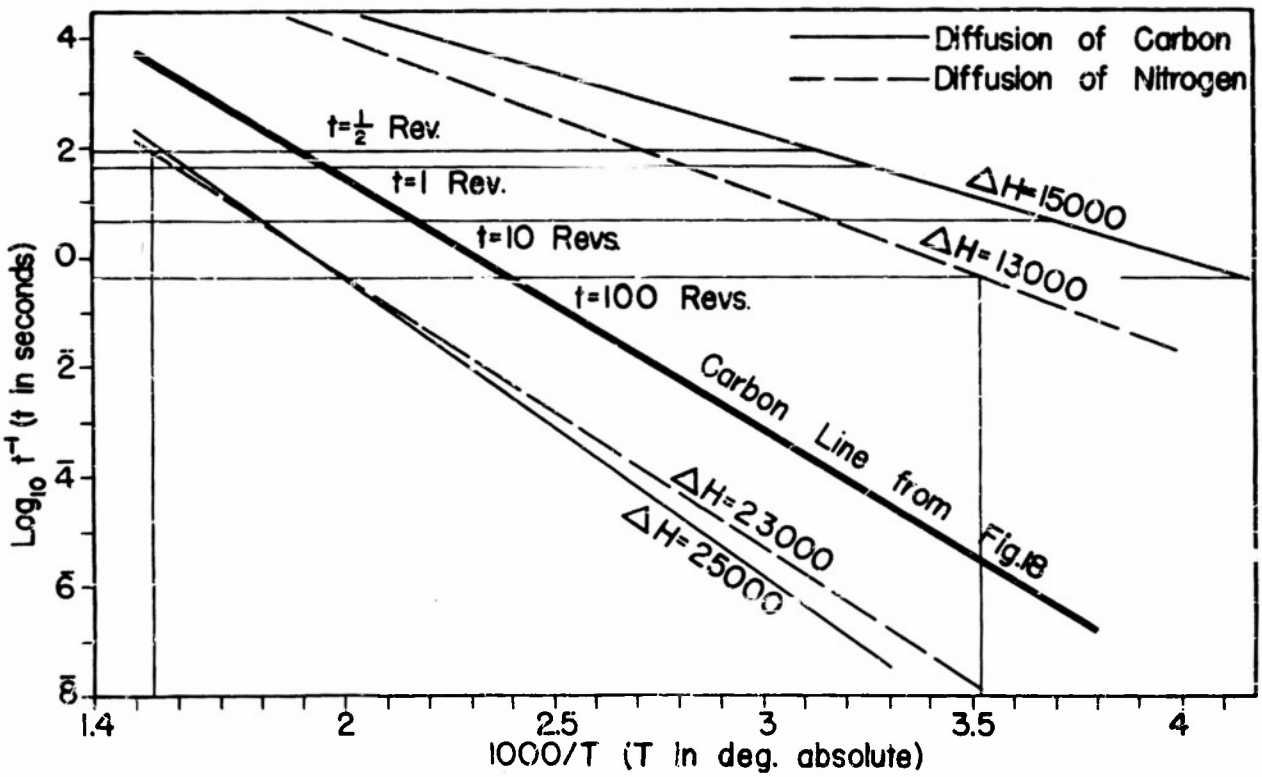

Fig.19 Effect of Variation of ΔH and t on the Temperature for Peak Life

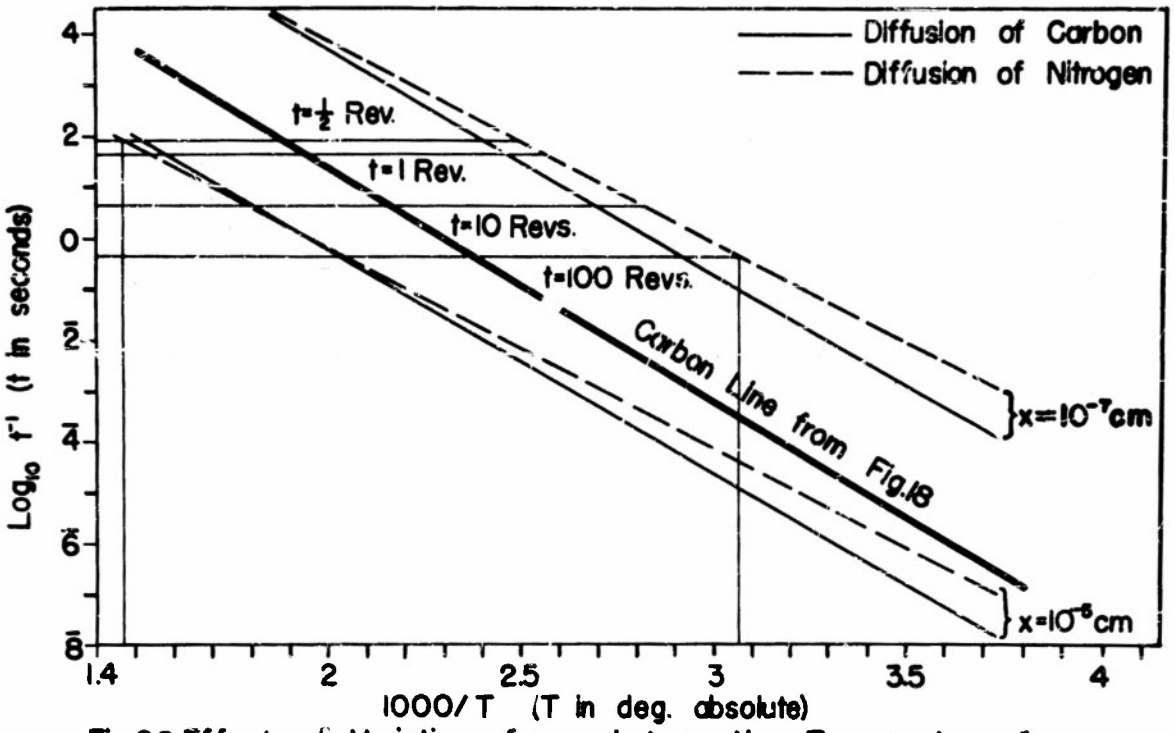

Fig.20 Effect of Variation of x and f on the Temperature for Peak Life

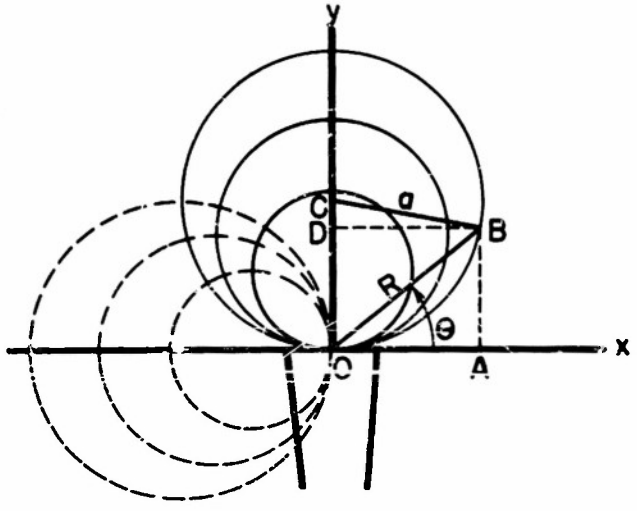

Fig.21 Approach of Solute Atoms to A Dislocation (after Cottrell[31])

Solid circles are equipotential lines. (Also below 0)

Broken circles are paths of approach of solute atoms (Also to right of 0)

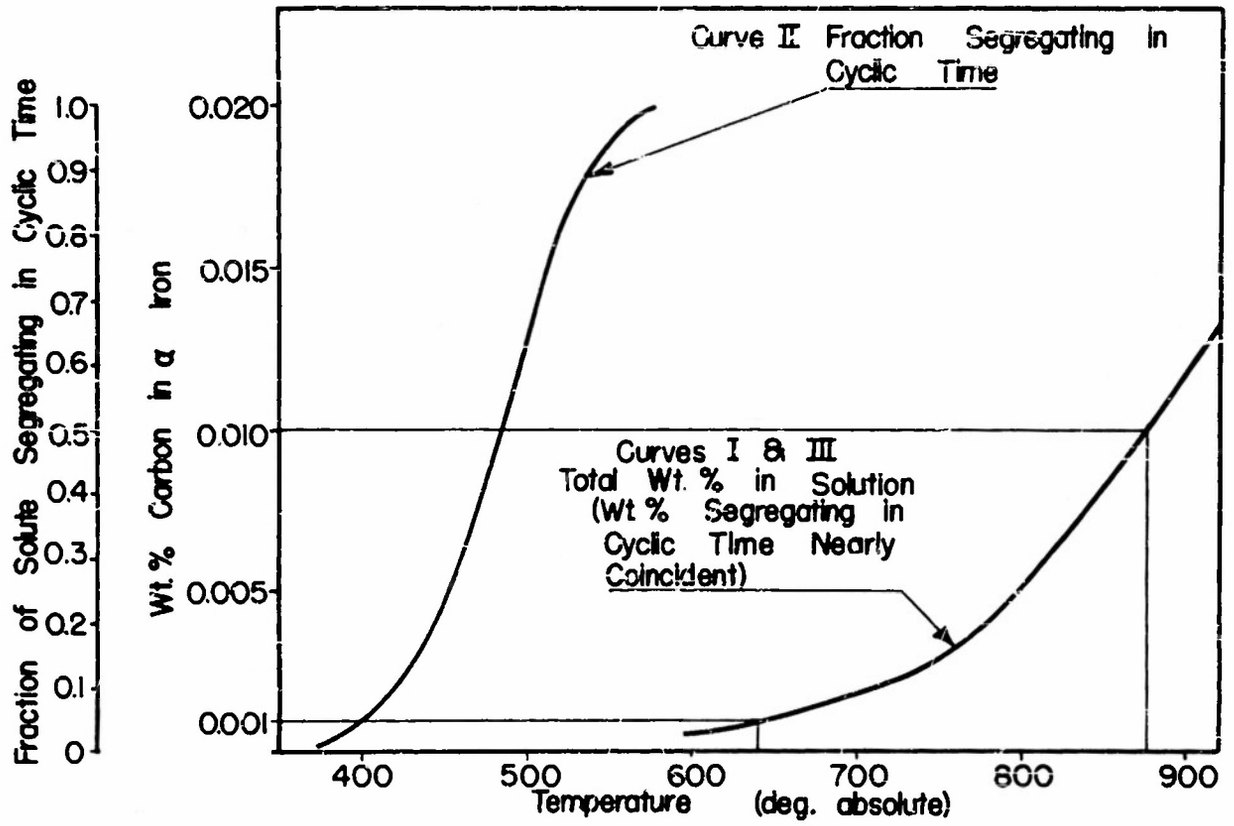

Fig.22 Segregation of Carbon to Dislocations During Strain Aging

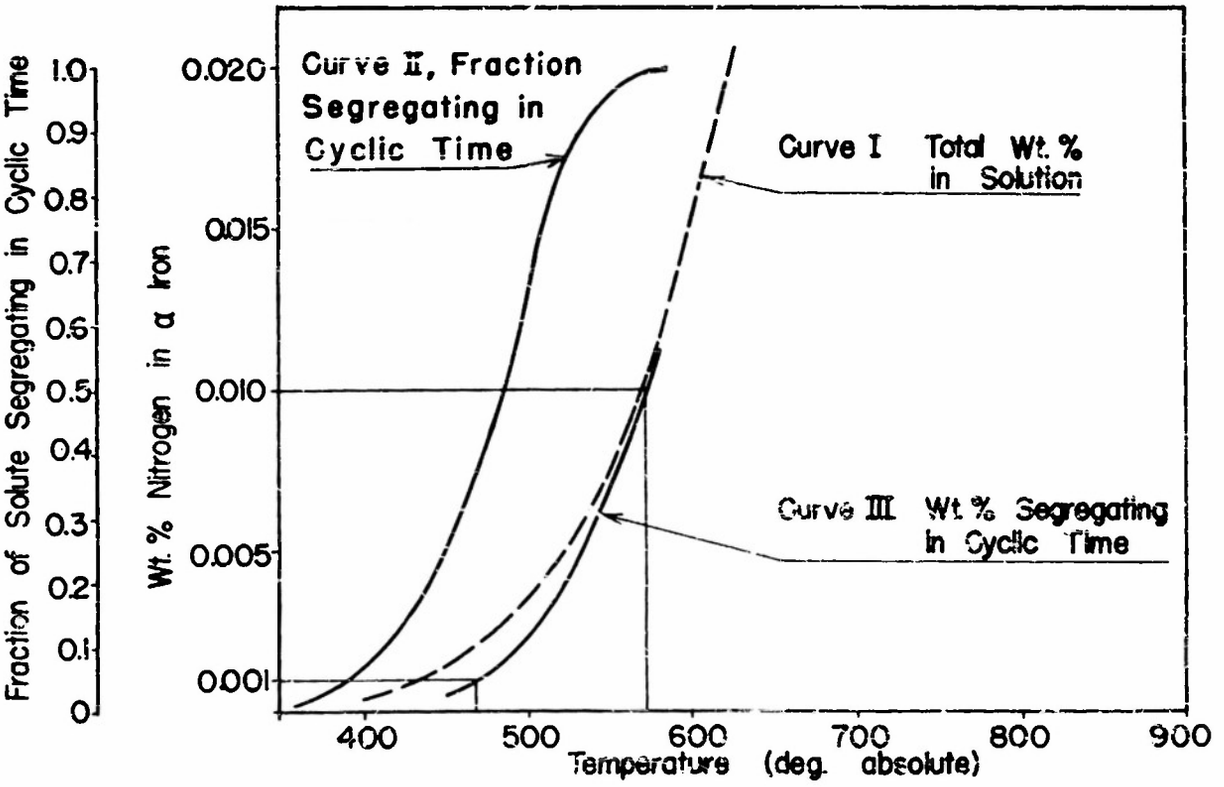

Fig.23 Segregation of Nitrogen to Dislocations During Strain Aging

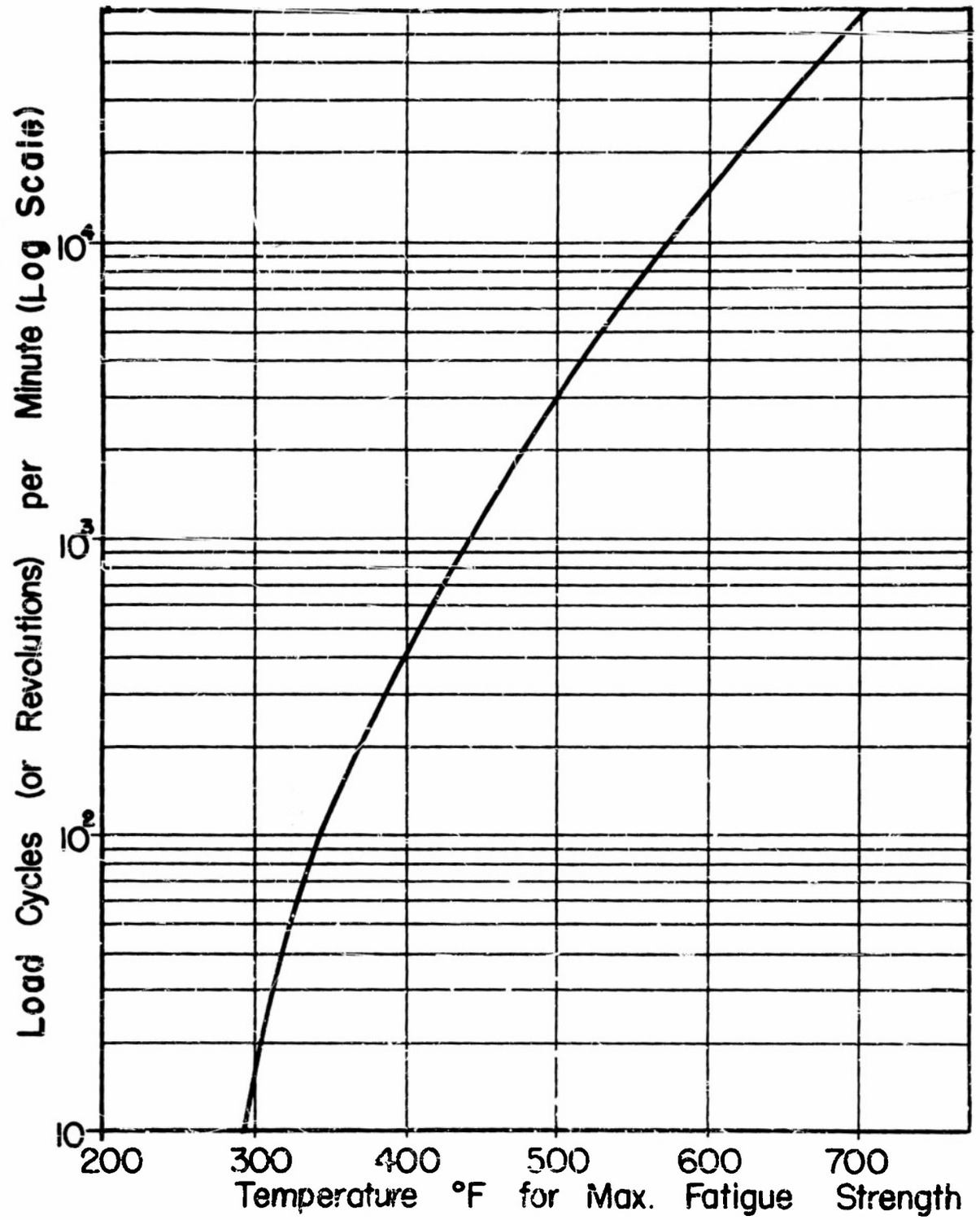

Fig.24 Predicted Effect of Speed on Operating Temperature for Maximum Fatigue Strength Due To Strain Aging